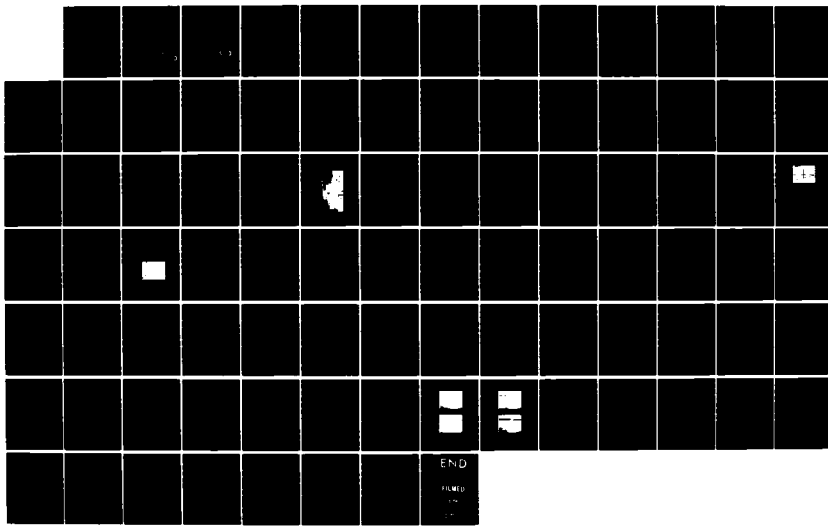
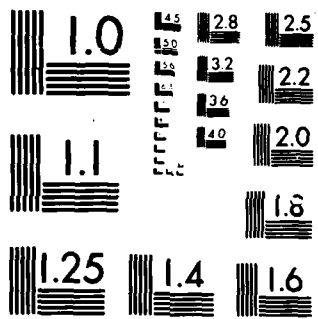


AD-A163 992 FLAT PLATE AND TURBINE VANE CASCADE HEAT TRANSFER 1/1  
INVESTIGATION USING A S. (U) AIR FORCE INST OF TECH  
WRIGHT-PATTERSON AFB OH SCHOOL OF ENGI. P K FILLINGIM  
UNCLASSIFIED DEC 85 AFIT/GAE/RA/85D-7 F/G 28/4 NL



END

FORMED  
1974  
GAE



MICROCOPY RESOLUTION TEST CHART  
NATIONAL BUREAU OF STANDARDS 1967 A

I

AD-A163 992



FLAT PLATE AND TURBINE VANE CASCADE  
HEAT TRANSFER INVESTIGATION  
USING A SHOCK TUBE

THESIS

Patrick K. Fillingim  
Captain, USAF

AFIT/GAE/AA/85D-7

DISTRIBUTION STATEMENT A

Approved for public release  
Distribution Unlimited

DTIC ELECTED  
FEB 13 1986  
**S** **D**

AMIC FILE COPY

DEPARTMENT OF THE AIR FORCE  
AIR UNIVERSITY

**AIR FORCE INSTITUTE OF TECHNOLOGY**

Wright-Patterson Air Force Base, Ohio

6 2 12 047

AFIT/GAE/AA/85D-7

FLAT PLATE AND TURBINE VANE CASCADE  
HEAT TRANSFER INVESTIGATION  
USING A SHOCK TUBE

THESIS

Patrick K. Fillingim  
Captain, USAF

AFIT/GAE/AA/85D-7

DTIC  
ELECTED  
FEB 13 1986  
**S D**  
B

Approved for public release; distribution unlimited

AFIT/GAE/AA/85D-7

FLAT PLATE AND TURBINE VANE CASCADE  
HEAT TRANSFER INVESTIGATION  
USING A SHOCK TUBE

THESIS

Presented to the faculty of the School of Engineering  
of the Air Force Institute of Technology  
Air University  
In Partial Fulfillment of the  
Requirements for the Degree of  
Master of Science in Aerospace Engineering

Patrick K. Fillingim, B.S., M.B.A.

Captain, USAF

December 1985

Approved for public release; distribution unlimited

## ACKNOWLEDGEMENTS

This project would never have been possible without the talents of a very special group of people. In particular, I am especially indebted to: Dr. William C. Elrod, my thesis advisor, for his assistance, guidance and exceptional good humor during some of my trying times and Dr. James Hitchcock for his assistance on the flat plate theory analysis. I am also grateful for the support and stupendous work performed by Mr. Nicholas Yardich, the lab supervisor, and his staff, Mr. Leroy Cannon, and Mr. Jay Anderson. The experimental piece of work would not have been possible without the superior and talented AFIT Shop personnel lead by Mr. Carl Shortt. I would also like to thank Lt. John Gochenaur, who performed the preliminary investigation of this problem and was available to handle some of my questions. For the equally important support given by my fellow students through their friendship, good-naturedness and technical advice, I thank you all.

Patrick K. Fillingim

Decision For	
1. GRADE	<input checked="" type="checkbox"/>
2. TIP	<input type="checkbox"/>
3. Commend	<input type="checkbox"/>
4. Certification	<input type="checkbox"/>
Comments	
Classification	
Availability	
Available	Not Available
Dist	Special
A-1	

## Table of Contents

	Page
Acknowledgements . . . . .	ii
List of Figures . . . . .	v
List of Symbols . . . . .	vii
Abstract . . . . .	ix
I. Introduction . . . . .	1
Background . . . . .	1
Objectives and Scope . . . . .	3
II. Theory . . . . .	5
Shock Tube Principles . . . . .	5
Heat Transfer and the Thermal Boundary Layer . . . . .	7
Flat Plate Solution . . . . .	8
Turbine Vane Solution . . . . .	12
Heat Transfer Measurement . . . . .	14
Flow Visualization . . . . .	16
III. Experimental Apparatus . . . . .	19
Hardware . . . . .	19
Shock Tube . . . . .	19
Shock Reflection Section . . . . .	19
Cascade Test Section . . . . .	21
Flat Plate Section . . . . .	23
Instrumentation . . . . .	23
Pressure Transducers . . . . .	23
Germanium Thermocouple . . . . .	24
Heat Flux Gages . . . . .	25
Schlieren Flow Visualization System . . . . .	26
IV. Experimental Procedures and Data Reduction . . . . .	27
Flat Plate Data . . . . .	27
Turbine Vane Data . . . . .	29
V. Results and Discussion . . . . .	31
Flat Plate Heat Transfer . . . . .	31
Turbine Vane Heat Transfer . . . . .	47
Flow Visualization . . . . .	62

	Page
VI. Conclusions . . . . .	66
VII. Recommendations . . . . .	67
Appendix A: Germanium Thermocouple . . . . .	69
Appendix B: Equipment . . . . .	71
Bibliography . . . . .	72
Vita . . . . .	75

## List of Figures

Figure		Page
1	Shock Tube Wave Phenomena . . . . .	6
2	Flow Over a Splitter Plate After the Shock Wave Has Passed the Leading Edge . . .	8
3	Heat Transfer Model For Gage Substrate . . . . .	14
4	Schlieren System . . . . .	18
5	AFIT Shock Tube Apparatus . . . . .	20
6	Cascade Test Section Schematic . . . . .	22
7	Test Vane Profile and Instrument Locations . .	25
8	Thermocouple Output Trace for Flat Plate ( $U_{\infty} = 536 \text{fps}$ ) . . . . .	28
9	Thermocouple Trace and Transition Region . . .	31
10	Flat Plate Heat Transfer ( $U_{\infty} = 172 \text{fps}$ ) . . . . .	34
11	Flat Plate Heat Transfer ( $U_{\infty} = 214 \text{fps}$ ) . . . . .	35
12	Flat Plate Heat Transfer ( $U_{\infty} = 216 \text{fps}$ ) . . . . .	36
13	Flat Plate Heat Transfer ( $U_{\infty} = 216 \text{fps}$ ) . . . . .	37
14	Flat Plate Heat Transfer ( $U_{\infty} = 284 \text{fps}$ ) . . . . .	38
15	Flat Plate Heat Transfer ( $U_{\infty} = 407 \text{fps}$ ) . . . . .	39
16	Flat Plate Heat Transfer ( $U_{\infty} = 536 \text{fps}$ ) . . . . .	40
17	Flat Plate Heat Transfer ( $U_{\infty} = 351 \text{fps}$ ) . . . . .	41
18	Flat Plate Heat Transfer ( $U_{\infty} = 289 \text{fps}$ ) . . . . .	42
19	Flat Plate Heat Transfer ( $U_{\infty} = 470 \text{fps}$ ) . . . . .	43
20	Turbine Vane Heat Transfer ( $U_{\infty} = 164 \text{fps}$ ) . . . . .	48
21	Turbine Vane Heat Transfer ( $U_{\infty} = 211 \text{fps}$ ) . . . . .	49
22	Turbine Vane Heat Transfer ( $U_{\infty} = 283 \text{fps}$ ) . . . . .	50

Figure		Page
23	Turbine Vane Heat Transfer ( $U_{\infty} = 489 \text{fps}$ ) . . . . .	51
24	Turbine Vane 1/2 Chord Suction Side Heat Transfer . . . . . . . . . . .	52
25	Turbine Vane 1/12 Chord Suction Side Heat Transfer . . . . . . . . . . .	53
26	Turbine Vane 1/2 Chord Suction Side Heat Transfer . . . . . . . . . . .	54
27	Turbine Vane 1/2 Chord Suction Side Heat Transfer . . . . . . . . . . .	55
28	Turbine Vane 3/4 Chord Suction Side Heat Transfer . . . . . . . . . . .	56
29	Turbine Vane 3/4 Chord Suction Side Heat Transfer . . . . . . . . . . .	57
30	Turbine Vane 1/4 Chord Suction Side Heat Transfer . . . . . . . . . . .	58
31	Boundary Layer Visualization . . . . .	64
32	Germanium Surface Thermocouple . . . . .	70

List of Symbols

Symbol	Description	Units
C <sub>f</sub>	Coefficient of Friction	
C <sub>p</sub>	Constant pressure specific Heat	Btu/lbm- F
h	Heat transfer coefficient	Btu/sq.ft-s- F
k	Ratio of specific heats, Thermal Conductivity	Btu/hr-ft- F
M	Mach number	
Nu	Nusselt number	
P	Pressure	psia
Pr	Prandtl number	
q	Heat flux	Btu/sq.ft-sec
r	Recovery factor	
Re	Reynolds number	
t	time	sec
T	Temperature	F or R
U	Velocity	. ft/sec
x	x-axis position	ft
$\alpha$	Laminar Transition factor	

Symbol		Units
<b>Subscripts</b>		
aw	Adiabatic wall	
i	Denotes cascade inlet conditions	
ii	Denotes cascade outlet conditions	
n	Number of finite element divisions	
s	Incident shock	
w	Wall	
oo	Freestream	
<b>Superscripts</b>		
*	Reference state	
<b>Greek Letters</b>		
$\tilde{\tau}$	Time integration variable	sec

ABSTRACT

A shock tube was used to initiate boundary layer growth on a splitter plate at zero incidence. The heat transfer rate determined from a thin film semiconductor gage was compared to theoretical values for the flat plate heat transfer problem. The correlation between the theoretical laminar and turbulent boundary layer equations and the experimental data for various shock Mach number flows showed excellent agreement.

The shock tube was also used to generate high temperature gas flows which were allowed to pass through a turbine vane cascade. Thin film semiconductor and resistance gages were used to provide temperature histories at four locations along the suction side of a turbine vane over a range of shock strengths. Heat transfer rates were determined from these temperature histories using a finite differencing scheme to approximate the energy equation for a semi-infinite solid. The investigation showed that the rate of heat transfer along the suction side of the vane decreased with chordwise position from the stagnation point at the leading edge to the half chord position. At the three quarter chord position, the heat transfer rates were found to be higher than the preceding

chord points.

Flow visualization was provided using a schlieren system. Photographs were taken showing boundary layer transition from laminar to turbulent flow for sonic flows over a flat plate.

FLAT PLATE AND  
TURBINE VANE CASCADE  
HEAT TRANSFER INVESTIGATION  
USING A SHOCK TUBE

I. Introduction

To obtain increased performance and improved fuel efficiency, gas turbine engineers are constantly striving to raise the turbine inlet temperatures at which their engines operate. In order to accommodate these high temperatures and improve component life, it is necessary to understand the heat transfer mechanisms involved in this hostile environment. Consequently, the effects of various factors on the rate of heat transfer to the components of a gas turbine hot section have been under experimental scrutiny for a number of years.

Background

A number of papers are available in the literature concerning the measurement of heat transfer in shock tube facilities. Felderman (1968) examined the passage of an initial shock wave over a semi-infinite flat plate within a shock tube. Curves were presented showing the time required to reach steady state for a given flow condition and model size. Davies and Berstein (1969) investigated the heat transfer and transition to turbulence in the shock-induced

boundary layer over a flat plate. They showed that for a laminar boundary layer with zero pressure gradient the flow is substantially steady where  $\alpha = 0.3$ . This nondimensional alpha was calculated from the equation:  $\alpha = x/(U_c^* t)$ , where  $U_c^*$  was the gas flow velocity,  $x$  was the fixed position on the plate from the leading edge, and  $t$  was the time measured once the gas flow velocity had passed the leading edge. A more recent study by Abbott, Liu, and Walker (1973) attempted to formulate the solution of a boundary layer on a splitter plate through a finite differencing scheme. An important result from these calculations concerns the asymptotic approach of the boundary layer to steady state at a particular axial location on the splitter plate using the inverse of Davies' and Bersteins' alpha as the transition requirement. Dunn and Stoddard (1977) conducted heat transfer experiments in a shock tube with a test section designed to approximate the geometry of the entrance to a turbine stator stage. They demonstrated transient test techniques to obtain "spatially resolved heat-transfer rates on gas turbine components". Using thin-film heat-transfer gages, they observed a local hot spot near the leading edge on the suction side of their test airfoils. This local hot spot was later investigated by Gochenaur (1984) in comparison with other positions along the vane.

### Objectives and Scope

The purpose of this study was to experimentally investigate the rate of heat transfer to a flat plate and a turbine vane cascade using a shock tube to establish a high temperature flow and to observe the associated thermal boundary layer. The specific objectives were:

1. To expand the heat transfer data base for a flat plate in the form of a splitter plate. This included establishing confidence in the measurement technique through comparison of the experimental data with theoretical solutions and visualizing the transition from laminar to turbulent boundary layer flow at low Mach numbers through a schlieren optical network.
2. To develop the experimental technique and data analysis procedures for use of the shock tube in research on turbine vane heat transfer.

The flows generated in this study were by no means identical to what would be encountered in a gas turbine hot section. The flow medium used was atmospheric air, not a mixture of combustion products. Additionally, the total pressures and temperatures generated were not as high as might be found in a typical turbine engine. However, the ratios of the flow temperatures to the turbine vane surface temperatures were indicative of those in an operational gas turbine. Heat transfer rates were determined at three locations along the

surface of each of two instrumented vanes over a range of temperature ratios. The schlieren flow visualization investigation was used to establish correlation between the heat transfer rates and the development of a boundary layer on a flat plate surface.

In this study, attention was given to the establishment of a boundary layer flow along a flat plate behind an initiating shock wave and developing experimental techniques for investigating heat transfer within a turbine vane cascade. Using a shock tube enabled a quasi-steady flow to be generated for a short time at the desired temperature and pressure for simulating a heat transfer distribution. Recent developments in thin film resistance heat flux gage technology have made it possible to measure temperature differences on the order of  $0.1^{\circ}\text{F}$ . This was important for some of the low Mach number runs made during this study.

## II. THEORY

### Shock Tube Principles

The high temperature, high pressure flows required for this study were produced using a shock tube. This shock tube consisted of a high pressure driver section and a relatively low pressure driven section separated by a diaphragm (See figure 1). When the diaphragm dividing these two regions was ruptured, a shock wave developed which propagated into the driven section as shown in figure 1. As the shock wave traveled into the driven section, a rarefaction wave simultaneously propagated into the driver section at the local sonic velocity. There was a static pressure and temperature rise across the shock wave, and a velocity was imparted in accordance with the standard normal shock relations. Upon reaching the far end of the shock tube, the incident shock wave was reflected and propagated back into region 2, causing an additional pressure and temperature rise while bringing the flow to rest, region 5 in figure 1. This region provided the test conditions for the turbine vane cascade experimentation. For the flat plate tests, which were conducted behind the incident shock wave, the test conditions and test time relate to region 2. In this manner, a high temperature and pressure region was created easily and with little operating expense. Also, it should be noted that though regions 2 and 3 have the same pressure and velocity, region 3 was established through

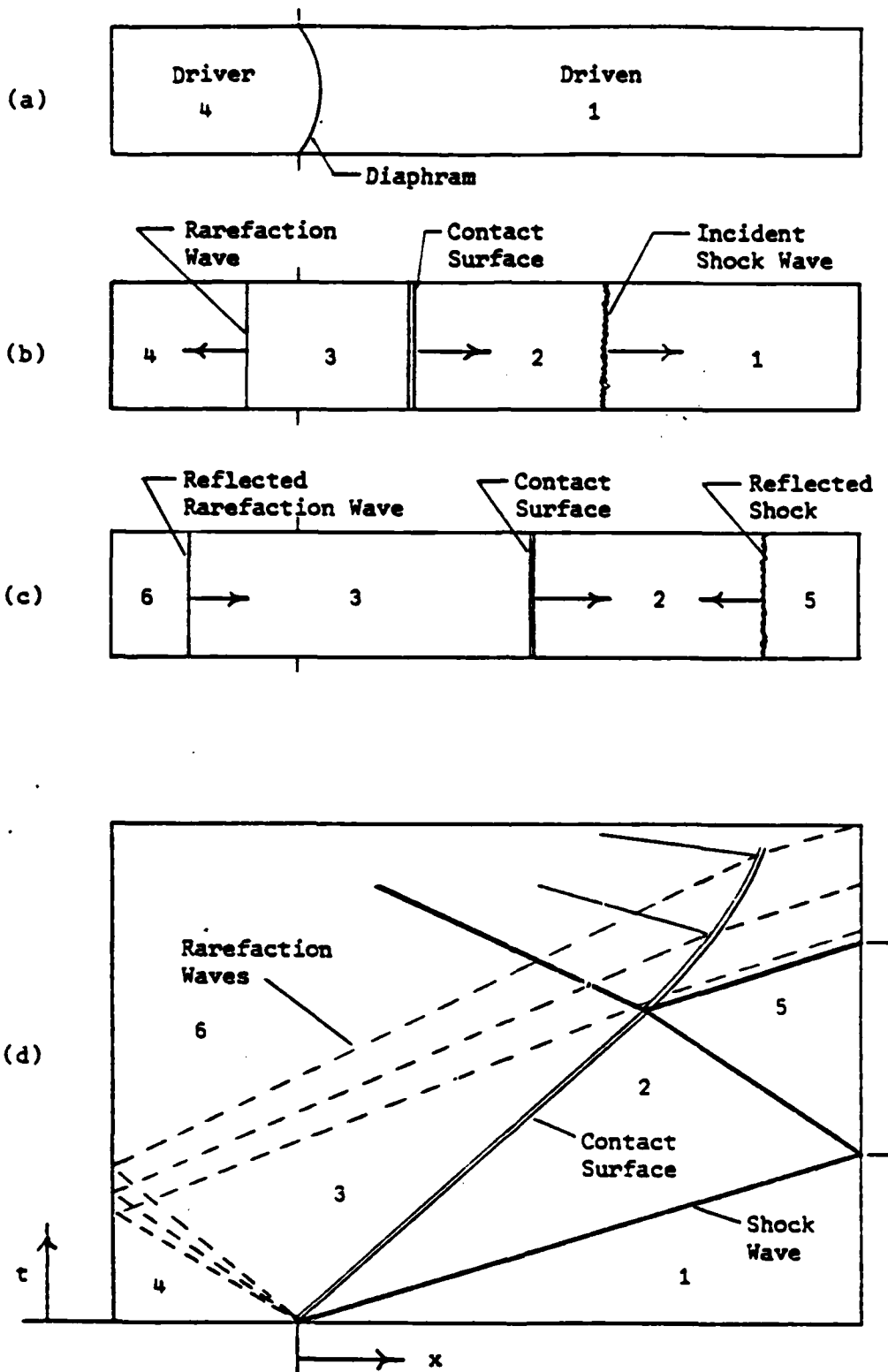


Figure 1: Shock Tube Wave Phenomena

isentropic expansion while region 2 resulted from a highly viscous shock event, so that a temperature discontinuity existed between them in the form of contact surface, C. (Chapman, 1971)

The primary constraint associated with using the shock tube was the limited duration of the desired flow conditions. Typically, available test times are on the order of 2 to 10 milliseconds. The reason for these short test times can best be explained by figure 1 which applies to the case where a test section was located at the far end of the driven section. As depicted in the figure, the available test time was the interval between the arrival of the incident shock wave and the next subsequent disturbance. This second disturbance was either the reflection of the rarefaction wave from the driver section end wall or a reflection from the contact discontinuity of the shock wave which is propagating back into region 2 (Shapiro, 1954). Determination of which of these secondary waves reached the test apparatus first is not intuitive, but requires analysis of the given flow conditions.

#### Heat Transfer and the Thermal Boundary Layer

The high temperature, high speed flows generated by the shock tube cause the formation of a thermal boundary layer over the side walls of the tube itself as well as over the turbine vanes of the test section cascade. This very thin layer in the neighborhood of a body becomes the flow region

where the temperature varies from that of the freestream to that of the surface. Mathematical solutions for the rate of heat transfer through this boundary layer are limited to a few simplified cases. For purposes of this study, the numerical solutions for laminar flow over a flat plate and an empirical solution for turbulent flow are of interest. These solutions are discussed in detail by a number of authors (i.e. Glass, Schlichting, and Kays and Crawford), thus only the pertinent points will be discussed here.

Flat Plate Solution. The formation of a boundary layer behind a moving normal shock along a flat plate is illustrated by figure 2.

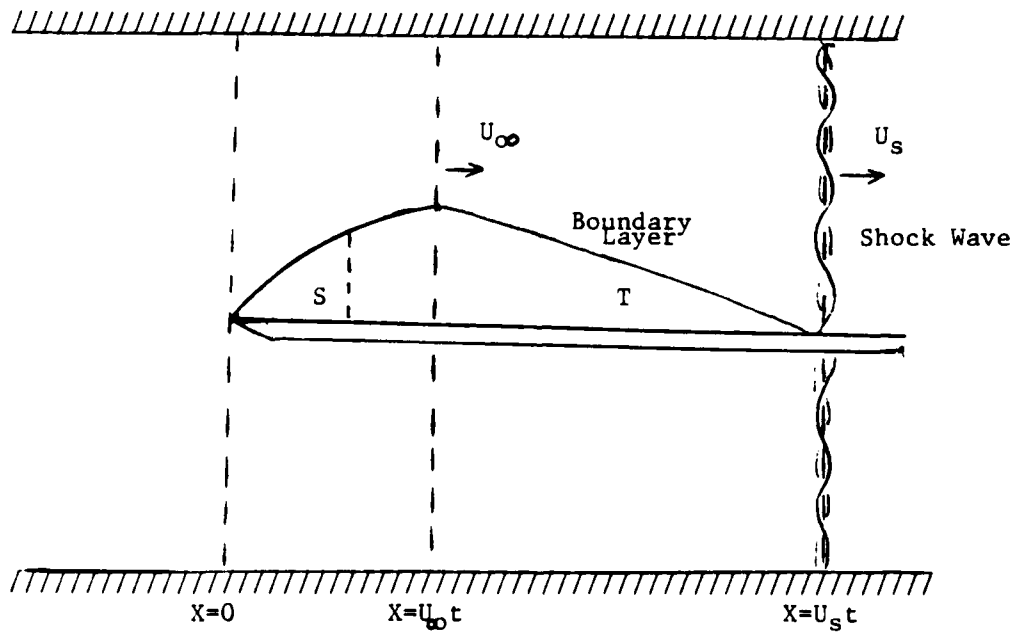


Figure 2: Flow Over a Splitter Plate After the Shock Wave Has Passed the Leading Edge

The passage of a normal shock through a shock tube results in the formation of a non-steady boundary layer along the tube sidewalls and flat plate. Schlichting pointed out that the resulting boundary layer is similar to but slightly thicker than that corresponding to an impulsively started flat wall (Schlichting, 1979). Abbott used a finite difference scheme to describe the development of the boundary layer between the leading edge of a splitter plate and the shock wave. An important result from those calculations concerns the asymptotic approach of the boundary layer to steady state at a particular axial station on the splitter plate. This information is important to shock tube experimentalists who employ splitter plates for optical flow field visualization (Abbott, 1973).

In order to obtain an estimate of the heat transfer for purposes of this study, the problem was treated as a high speed flow over an isothermal flat plate. The assumption of constant wall temperature has been shown to be valid for laminar flow (Schlichting, 1979). It has also been found to be quite reasonable for turbulent boundary layers except possibly for those initiated by strong shocks (Glass, 1958). Using this analysis, the rate of heat transfer from the flow over a flat plate is given by,

$$q = h(T_{Aw} - T_w) \quad (1)$$

where  $h$  is the local heat-transfer coefficient,  $T_{aw}$  is the adiabatic wall temperature and  $T_w$  is the temperature of the flat plate. The adiabatic wall temperature can be written,

$$T'_{aw} = T_\infty + r^2 U_\infty^2 / 2 C_p \quad (2)$$

in which  $T_\infty$  is the free stream static temperature,  $C_p$  is the constant pressure specific heat, and  $U_\infty$  is the free stream flow velocity. The recovery factor,  $r$ , for a turbulent boundary layer, is the cube root of the Prandtl number,  $Pr$ , whereas  $r$  is the square root of  $Pr$  for laminar flow.

Since the shock wave in a shock tube moves at a much higher velocity than does the air behind it, two boundary layer developments on the flat plate are of interest. A velocity is imparted to the air behind the shock wave and this air moving over a surface initiates the development of a boundary layer immediately behind the shock. This initiating point moves with the shock, therefore the boundary layer develops at a particular location in proportion to the velocity of the air behind the shock,  $U_\infty$ , and the time elapsed since the shock passed. Accordingly, this is a transient boundary layer. The other boundary layer develops beginning at the leading edge of the plate as a result of the same air velocity over the plate,  $U_\infty$ , but its characteristics are dependent on only distance from the leading edge. This is a steady state boundary layer.

In the development of the flat plate boundary layer at some distance  $x$  from the leading edge, the transient boundary layer moving with the incident shock wave dominates the heat transfer until  $U_{\infty}^* t$  is one to three and a third times greater than  $x$ . After which, the dominance will be transferred to the steady boundary layer which developed from the leading edge. The transient region, region T of figure 2, is governed by the equations developed by H. Mirels (1956). The steady state boundary layer which is an application of Prandtl's boundary layer theory discussed by H. Blasius (1908), corresponds to region S of figure 2.

The steady heat-transfer coefficient in Eqn. (1) can be related to the steady local Nusselt number  $Nu_x$ , position  $x$ , and thermal conductivity  $k$  by,

$$\frac{h}{k} = Nu_x \frac{k}{x} \quad (3)$$

where, for laminar boundary layers

$$Nu_x = 0.352 Re^{0.5} Pr^{0.75} \quad (4)$$

and, for turbulent boundary layers

$$Nu = 0.029 Re^{0.8} Pr^{0.5} \quad (5)$$

The flow properties such as  $k$ ,  $C_p$ , and  $Pr$ , were evaluated at a reference temperature,  $T^*$ , for both laminar and turbulent

flow. The reference temperature was defined as,

$$T^* = \frac{T_\infty + T_w}{2} + 0.22(T_{Aw} - T_\infty) \quad (6)$$

The unsteady heat-transfer coefficient, i.e. no leading edge effect, can be related to the unsteady Nusselt number  $Nu_x$ , distance  $x = U_\infty t$ , time after shock passes gage  $t$ , and thermal conductivity  $k$  by,

$$h = Nu_x \cdot k / U_\infty \cdot t \quad (7)$$

where, for laminar boundary layers

$$Nu_x = 0.5 L_f^{5.2} Re^{0.8} Pr_w^{0.52} \quad (8)$$

and, for turbulent boundary layers

$$Nu_x = 0.024 Re^{0.8} Pr_w^{0.5} \quad (9)$$

The flow properties were evaluated at  $T_w$ . Since the Prandtl number was near unity, it was possible to resort to the compression wave approximation from Schlichting (1979) for the power of the Prandtl number used in Eqn. (8). The local skin-friction coefficient,  $C_f$ , is a function of the Reynolds number and the local flow velocity (Schlichting, 1979).

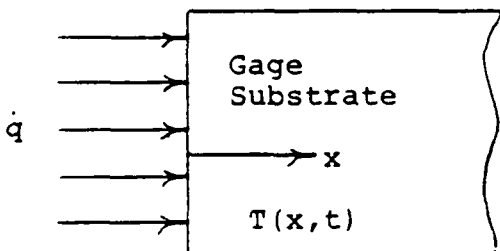
Turbine Vane Solution. The boundary layer development on the turbine vane in the shock tube is initiated at the vane stagnation point then gradually thickens as it travels chordwise along the vane. This boundary layer may or may not

become turbulent depending upon the character of the flow and the geometry of the passage between adjacent vanes. Analytic heat transfer solutions are not generally available for arbitrary vane geometries; however, numerical routines, such as STAN 5 (Crawford, 1976), are being refined to address this problem. Gochenaur (1984) found that his experimental data at the stagnation point of a vane in cascade compared well with the theoretical 2-dimensional analysis for the stagnation point on a cylinder in a uniform cross flow.

In the absence of a mathematical solution for the heat transfer over the entire turbine vane, qualitative predictions become significant. Flow characteristics which tend to stabilize the boundary layer and hence retard the transition to turbulence are of particular interest. For subsonic flow of a gas, heat transfer from the boundary layer to the wall is one condition which tends to forestall transition (Schlichting, 1979). This appeals to intuition since it results in an energy transfer from the boundary layer to the surface. Additionally, a favorable pressure gradient, such as that found on the pressure side of a turbine vane, also inhibits transition. Finally, while suction tends to stabilize the boundary layer, blowing tends to encourage instability. This latter case is of concern with turbine blades which utilize film cooling. Blowing was not considered in this study but could be incorporated in future studies.

### Heat Transfer Measurement

Utilizing the measured time history of the temperature of a surface which is suddenly exposed to a high temperature gas flow, the heat transfer can be calculated. In a shock tube, this temperature history may be determined by the use of a flush mounted short response-time transducer such as a thin film resistance gage or a semiconductor thermocouple. These gages are similar in that both utilize a thin film, often gold or platinum, vapor deposited on an insulating substrate with known thermal properties. Utilizing the known properties of the gage, the flat plate or vane surface temperature may be determined from voltage differences readable on an oscilloscope. For the purpose of calculating heat transfer, this substrate was modelled as a semi-infinite slab like the one shown in figure 3.



$\dot{q}$  = heat transfer rate  
 $k$  = thermal conductivity  
 $\rho$  = density  
 $c$  = specific heat  
 $T$  = temperature  
 $t$  = time

Figure 3: Heat Transfer Model For Gage Substrate

Assuming constant substrate properties, the heat equation

can be written,

$$\frac{\partial T(x,z)}{\partial t} = \frac{k}{\rho C_p} \frac{\partial^2 T(x,t)}{\partial x^2} \quad (10)$$

with initial and boundary conditions as follows.

$$T(x,0) = 0, x>0$$

$$q(0,t) = -k \frac{\partial T(x,t)}{\partial x}, t>0$$

$$T(x,\infty) = 0, t>0$$

(Bogdan, 1967; Kendall, 1966).

The solution is well detailed and results in the relation,

$$q(z,t) = \frac{1}{2} \left( \frac{\rho k}{\pi} \right)^{1/2} \left[ T(t) + \frac{1}{\pi} \int_0^t \frac{z^{1/2} T(\tau) - t^{1/2} T(\tilde{\tau})}{(t-\tilde{\tau})^{3/2}} d\tilde{\tau} \right] \quad (11)$$

where  $T(t)$  is the substrate surface temperature and  $\tilde{\tau}$  is an integration variable.

There are two common methods for evaluating Eqn. (11) to obtain heat transfer rates from a temperature-time history. The first involves the use of analog networks which convert a thermocouple's output signal directly to heat transfer rate information in real time. These circuits are quite involved and are discussed in detail in the literature (Schmitz, 1963; Bogdan, 1967). The second uses a finite differencing scheme to approximate the governing partial differential equation. Cook and Felderman (Cook, 1966) developed such a numerical relation to obtain heat transfer rates. The range of shock Mach numbers firmly established laminar as well as turbulent boundary layer growth over the flat plate. The numerical

scheme allowed the sudden step-rise increase of the shock-induced temperature discontinuity. The equation as derived by Cook and Felderman,

can be written as,

$$q(\bar{t}_N) = 2\left(\frac{\rho_{CK}}{\pi}\right)^{1/2} \left[ \frac{T_s(t_c)}{2t_N^{1/2}} + \sum_{i=1}^{N-1} \left[ \frac{T(t_i) - T(t_{i-1})}{(t_N - t_i)^{1/2} + (t_i - t_{i-1})^{1/2}} \right] + \frac{T_N - T_{N-1}}{(t_N - t_{N-1})^{1/2}} \right] \quad (12)$$

This was a general expression and made no assumptions about the form of the temperature function. The accuracy was limited by the discrete intervals into which the known temperature history was divided and digitized. This numerical method treated the data as a piecewise continuous linear function.

#### Flow Visualization

A schlieren system can provide valuable qualitative information about the flow through a test apparatus. The path of a light beam as it passes through the test section encounters an index of refraction which is dependent on the local density in the test section. When a light beam encounters a density gradient in the test section normal to the beam, the light beam is turned in the direction of increasing index of refraction. In most media this means that the light is bent toward the region of higher density or lower temperature.

Using the system shown in figure 4, a light source is at the focus of mirror M1. The resulting parallel light beam enters the field of disturbance in the test section. The

light is collected by a second mirror M2 and folded into the camera by the flat mirror M3. A knife edge is placed at the focus of mirror M2. The camera was located at the conjugate focus of the test section. The brighter areas of the image represent regions in the test section where the index of refraction (and thus usually density) increases in the direction away from the knife edge. Dark areas represent regions where the index of refraction increases in the direction opposite to that in which the knife edge points.

In a quantitative study, measurements of the illumination or contrast, usually of the image on a photographic negative, must be made. These are quite time consuming and the resulting accuracy has not usually warranted the effort. Thus, standard schlieren systems are usually employed for qualitative studies of a temperature or density field, although quantitative measurement of shock wave angle or positions can be made. For a more detailed explanation of this optical technique refer to Reference 2.

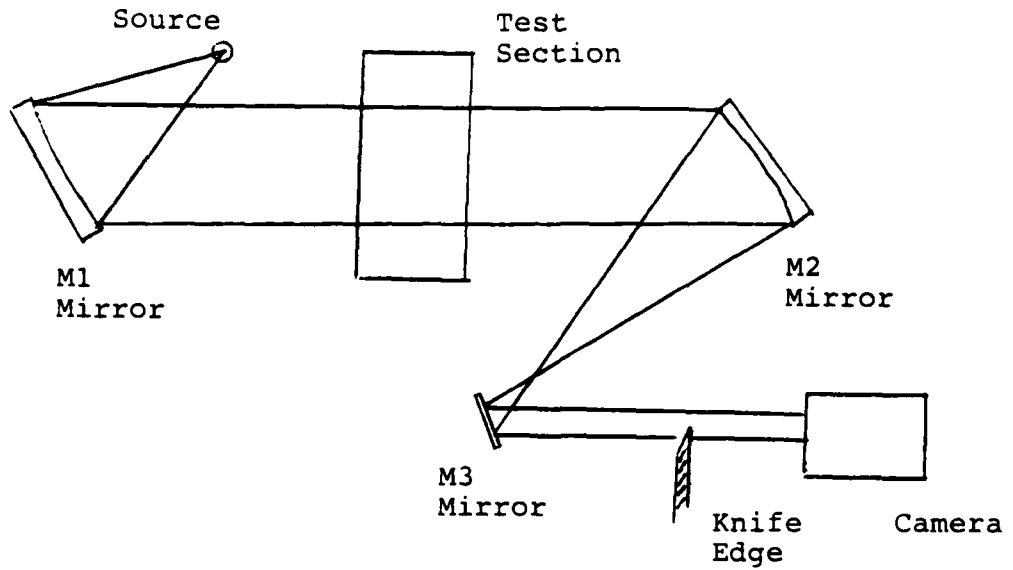


Figure 4: Schlieren system

### III. Experimental Apparatus

#### Hardware

Shock Tube. The main part of the experimental apparatus was the AFIT rectangular shock tube. The tube measured 16 feet (4.88 m) including a 4 foot (1.22 m) driver section, a 12 foot (3.66 m) driven section, each with a 4 in (10.15 cm) by 8 in. (20.32 cm) rectangular internal cross-section. The AFIT rectangular shock tube is described in detail by Ref. (13) and pictured in figure 5. A 100 psi air supply and a vacuum system were available for controlling pressure in the driver section and driven section, respectively. The driver section was hydraulically latched to the driven section. Mylar sheets, 0.002, 0.005, or 0.007 inch (0.054, 0.127, or 0.178 mm) thick were used to separate the two sections. Once the driver section was pressurized, the mylar sheet was ruptured by a pneumatic plunger mounted in the driver section. A pressure gage, calibrated from 0 to 200 inches (508 cm) of Mercury, mounted to the shock tube control panel was used to monitor the driver section pressure.

Shock Reflection Section. Bolted to the end of the driven section is a device designed to reflect an incident shock but allow the high pressure, high temperature gas of region 5 (see figure 1) to expand through the test section which was bolted

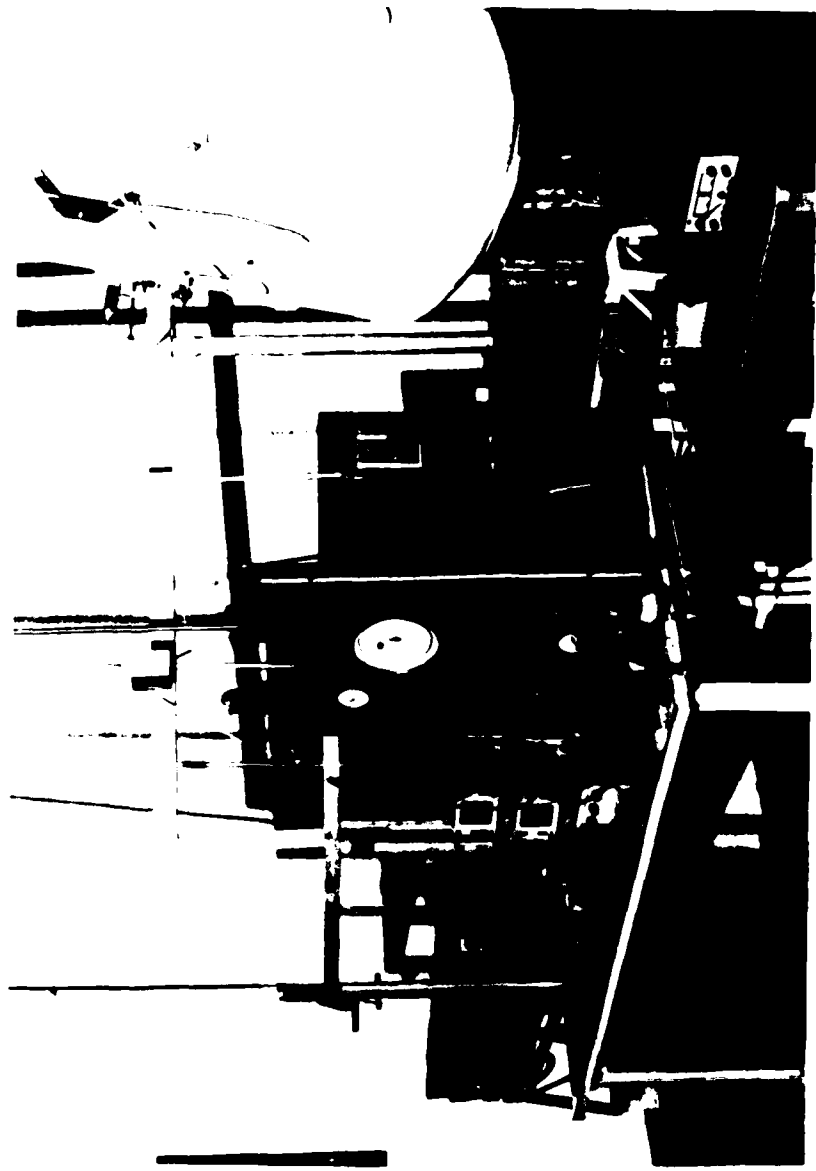


Figure 5: AFIT Shock Tube Apparatus

to the other side. The apparatus was described in a previous study (Gochenaur, 1984). The shock reflection section reflected the incident shock just as a second diaphragm would, but without the danger of producing mylar shrapnel which could damage delicate instrumentation.

Cascade Test Section. The cascade test section shown in figure 6 was bolted to the downstream end of the shock reflection section. Constructed primarily of 3/4 inch (1.905 cm) aluminum plate, it had plexiglass side walls to allow observation of the cascade itself. The profile of the aluminum test vanes was modelled after that of the General Electric CF6-50 first stage high-pressure turbine nozzle vanes. These vanes turned the flow through an arc of 75 degrees with a corresponding reduction in flow cross-section area from 8 sq-in (51.6 sq-cm) to approximately 2 sq-in (12.9 sq-cm), see figure 6. Seven vanes were mounted directly into the plexiglass side wall by means of steel pins. The heat transfer measurements were achieved through two specially instrumented vanes within the test section. Three thin-film resistance gages on each of two vanes provided temperature histories for various flow conditions. A thermocouple gage also provided additional suction side data.

Completing the test hardware, a 6 foot (1.83 m) long 2-1/2 foot (0.76 m) diameter dump tank suspended from the ceiling was bolted to the downstream flange of the cascade test

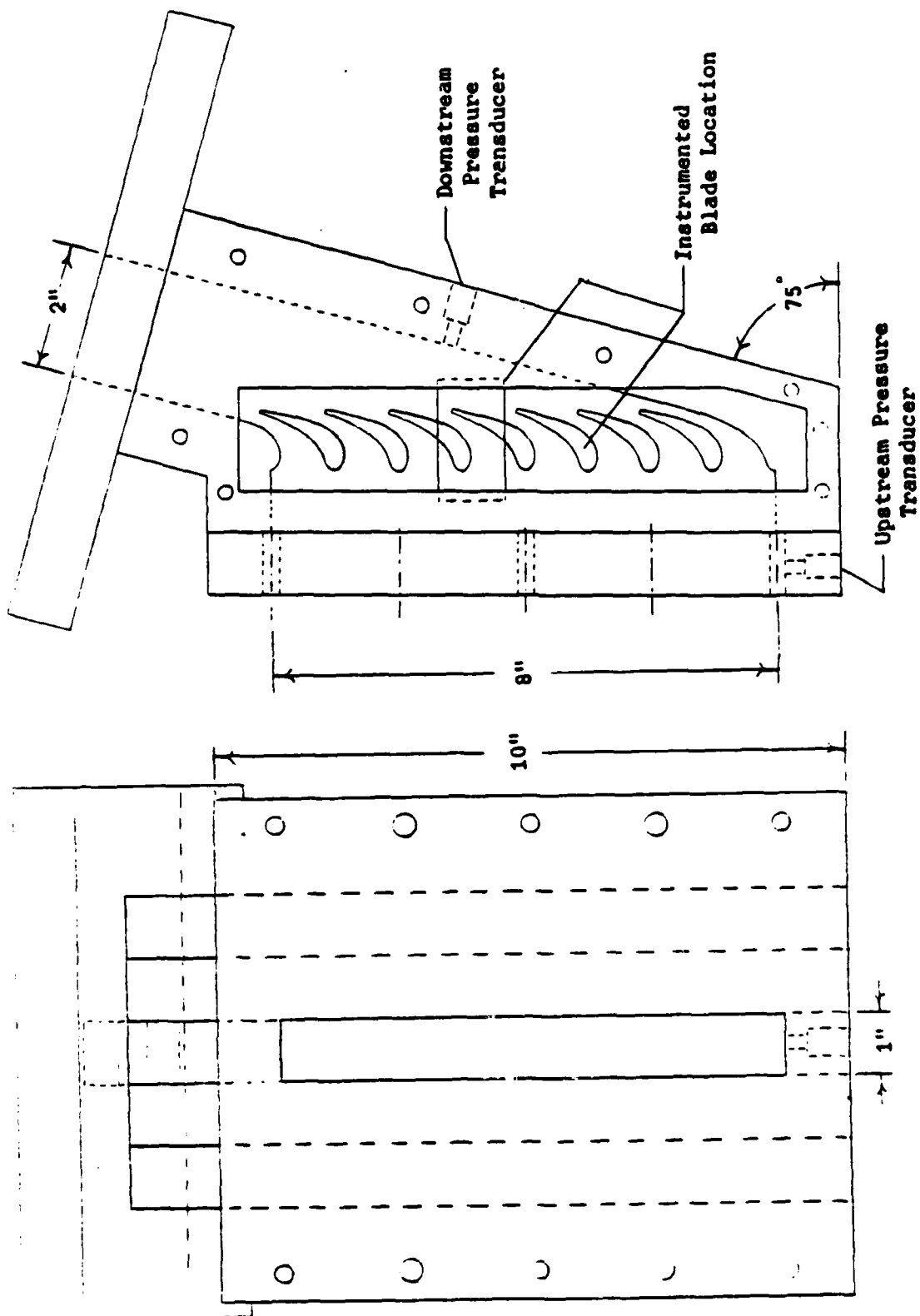


Figure 6 Cascade Test Section Schematic

section. This dump tank served to contain the overpressure and the noise associated with a shock wave.

Flat Plate Section. The flat plate was mounted in a 4 foot extension of the driven section without the shock reflection section. The 1/2 in (1.27 cm) thick by 4 in (10.16 cm) wide aluminum plate with a sharp leading edge and a 20 degree vertex angle was centered in the section to provide unobstructed flow of the air behind the incident shock wave and experience little interference from the shock tube walls. Data were obtained with the semiconductor thermocouple at one location on the flat plate, 2 inches (5.08 cm) from the leading edge. The section was fabricated with glass windows to permit schlieren photographs to be made.

#### Instrumentation

Pressure Transducers. Four Endevco pressure transducers were used in this study. An Endevco Model 8506-5 transducer, with a Kepco power supply providing the excitation voltage, was located in the shock tube 100 inches (254 cm) from the initial starting point of the shock wave. An Endevco Model 2501-500 transducer was located 40 inches (101.6 cm) downstream of the first transducer. This transducer served as the trigger for the oscilloscope and the schlieren spark lamp as required. Output signals from both of these transducers were routed through separate Honeywell amplifiers to the oscilloscope.

A pair of 8530A-100 pressure transducers were mounted in the lower wall of the cascade test section. One was positioned upstream of the cascade while the other was located downstream to measure the inlet and outlet static pressures, respectively. Both of these transducers were run by a single Endevco power supply while the output signal from each was amplified by its own Endevco Model 4423 signal conditioner. The output signals from these transducers were input to individual channels of the oscilloscopes. An oscilloscope camera with Polaroid film was used to capture the stored output trace after each run.

Germanium Thermocouple. Two Germanium Surface Thermocouples were used to measure the surface temperature histories required for the calculation of heat transfer rates. The attributes of these thermocouples which make them invaluable to shock tube research are their rapid response time and their ability to sense low heat rates (Kendall, 1968). The particular thermocouples used were developed by the McDonnell Company Engineering Laboratories for use in their Hypersonic Impulse Tunnel. See Appendix A for additional information.

For the flat plate studies, a thermocouple was mounted flush with the plate at 2 inches (5.08 cm) from the leading edge. For the cascade heat transfer investigation it was mounted flush with the surface of the turbine vane at the 1/4

chord point on the suction side. For all the cases, the thermocouple output was displayed on the oscilloscope.

Heat Flux Gages. Six heat flux gages, installed in two vanes, were acquired from CALSPAN Corporation for the measurement of heat transfer in the cascade test section. One vane was instrumented with three gages along the pressure side and another vane was instrumented with three gages along the suction side. The blade profile and the seven gage locations, six heat flux gages and one thermocouple, are illustrated in figure 7.

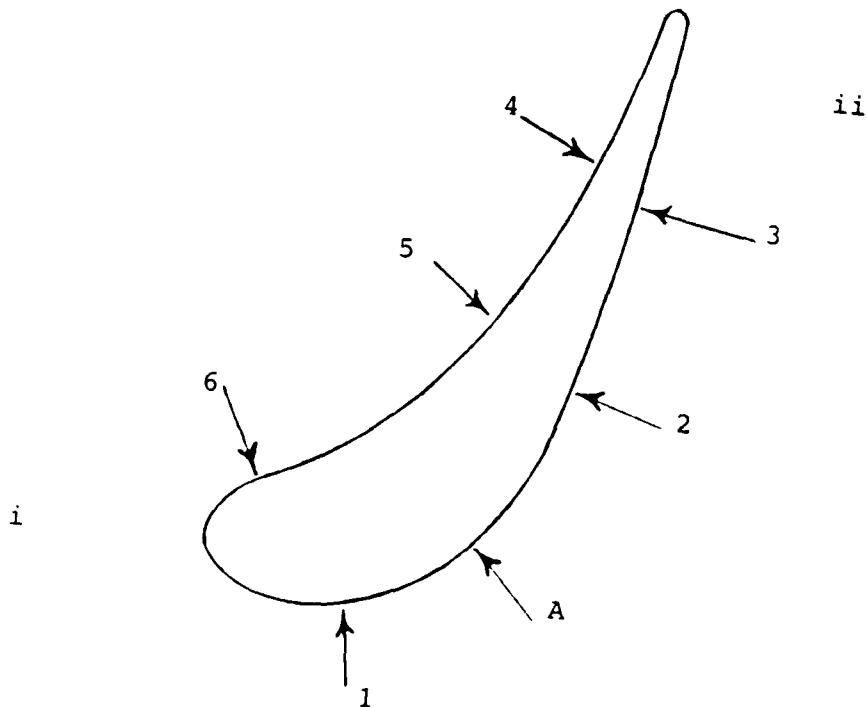


Figure 7: Test Vane Profile and Instrument Locations

Position	Gage type	Instrument Location
1	Heat Flux	1/12 chord,suction side
2	Heat Flux	1/2 chord,suction side
3	Heat Flux	3/4 chord,suction side
4	Heat Flux	19/24 chord,pressure side
5	Heat Flux	7/12 chord,pressure side
6	Heat Flux	1/8 chord,pressure side
A	Thermocouple	1/4 chord,suction side

Schlieren Flow Visualization System. In order to visualize the flow over the turbine vane cascade a schlieren system was positioned around the test section. A Cordin Model 5401 spark lamp was used to capture the boundary layer growth image on film. This spark lamp was triggered using the output from the Endevco Model 2501-500 pressure transducer located in the shock tube wall. This signal was delayed through the Cordin Model 435 time delay generator as required to study the flow through different stages of boundary layer growth. The image produced was captured on high speed (ASA 3000) Polaroid film using the box camera and mirror arrangement shown in figure 4.

#### IV. Experimental Procedure and Data Reduction

Prior to starting any of the experiments, the equipment was first allowed to warm-up. A mylar diaphram was then locked into the shock tube between the driver and driven section. Varying the driver and/or the driven section presure varied the strength of the shock generated by rupturing the diaphram. The driver pressure was operated from a minimum of 0 in-Hg gage to the maximum available supply pressure. The vacuum pump was used to partially evacuate the driven secton to a maximum of 17 in-Hg below barometric pressure. Finally, the ambient temperature and pressure were recorded prior to the set of runs.

##### Flat Plate Data

The Germanium thermocouple was located flush with the flat plate at 2 inches from the leading edge. The output trace from the gage was recorded on film by the oscilloscope camera. Figure 8 is a sample of one of these traces. For all flat plate runs the horizontal time scale was 1 millisecond per division (ms/div) while the vertical scale was varied from 5 millivolts per division (mv/div) to a maximum of 50 mv/div dependent on shock strength. As seen from the trace, the useful test time lasted about 7.0 ms from the initial thermocouple response until the arrival of a secondary disturbance (shock reflected from the driven end).

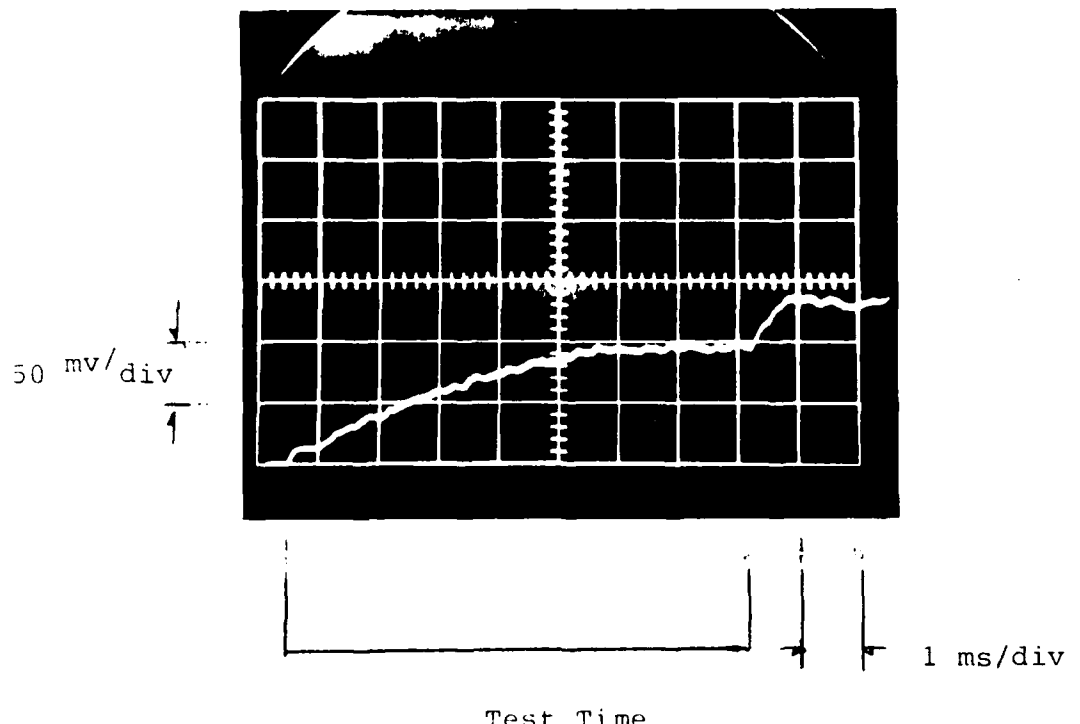


Figure 8: Thermocouple Output Trace for Flat Plate ( $U_\infty = 536 \text{fps}$ )  
 $(M = 1.32)$

The trace shows a short laminar region, approximately 0.5 ms, then transitions into a non-laminar boundary growth. Upon digitizing the voltage versus time curve using a Hewlett-Packard digitizer, the data were entered as an input file for a computerized reduction scheme. The computer program used the thermocouple's sensitivity (1.02 mv/ $^{\circ}\text{F}$ ) and the signal amplification to produce a temperature history from the input file. This temperature history was then analyzed using the finite differencing scheme of Eqn. (12) in order to

generate heat transfer rates. The initial rise in the thermocouple output trace corresponding to shock wave passage was important to the analysis of the cascade test section flow conditions presented in the next chapter

#### Turbine Vane Data

Heat Transfer data for the two turbine vanes were obtained in a similar manner to that for the flat plate. The cascade test section with two heat transfer gage instrumented vanes was installed. The heat transfer gages, manufactured and installed by CALSPAN Corporation, were mounted flush to the vane surfaces with the wire leads coming out the plexiglass sidewall of the test section. Another cascade test section utilizing an instrumented turbine vane with a thermocouple also provided data for various Mach number runs. The shock tube was operated over the range of driver pressures mentioned above with the driven section at barometric pressure. Based upon the conclusions reached in previous shock tube experimentation (Gochenaur, 1984), a shock reflection door was utilized to present a more uniform flow temperature to the vane by preventing the shock wave from entering the test section. The primary shock was reflected and the shock reflection section door opened initiating the flow of air from the shock tube (region 5) into the test section. The temperature history trace was digitized and analyzed using the same differencing scheme described for the flat plate data.

The useful quasi-steady flow test time was identified as the region during which the pressure transducer outputs are roughly constant. The pressure transducer outputs were stored on the oscilloscope trace simultaneously with the heat flux gages or thermocouple output for easy identification of the quasi-steady region of the flow. In order to satisfy the boundary conditions associated with Eqn. (12), the thermocouple trace had to be digitized from the point of initial high temperature flow, not just during the quasi-steady flow region.

## V. Results and Discussion

### Flat Plate Heat Transfer

The analytical solution used to obtain the theoretical heat transfer curves for these plots was acquired by initially solving for the laminar boundary layer equations and then at the appropriate transition point changing to turbulent boundary layer equations. This transition point was the region on the oscilloscope trace (see figure 9) where the steady laminar boundary layer made a sudden turn upwards signifying an abrupt change in flow conditions, i.e. turbulent boundary layer growth.

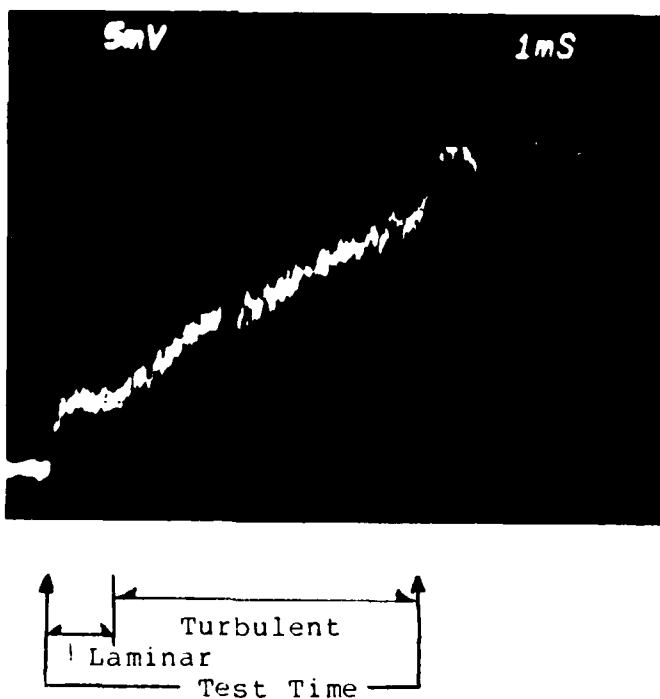


Figure 9: Thermocouple Trace and Transition Region

As the shock arrives there is a step-rise in temperature of the gas adjacent to the surface and a smaller jump in surface temperature. In theory the corresponding heat rate is infinite but there is rounding-off due to the finite shock thickness and gauge response time, but still the heat transfer rate is very large. Transitioning from laminar to turbulent flow necessitated the heat flux rate to be calculated from either the steady heat transfer coefficient derived from Eqn. (5) or the unsteady heat transfer coefficient derived from Eqn. (9). The laminar boundary layer transitioning to a turbulent boundary layer was indicated clearly by the flat plate run of figure 13. For the low Mach number runs the transient turbulent boundary layer calculations correlated well with the experimental data. However, in the Mach range of  $M=1.16$  and greater, the turbulent experimental data points behaved comparable to a steady turbulent boundary layer calculation. The two theoretical curves are plotted along with the experimental data for a better comparison. Future studies in this region could be looked at to better understand the transient effects prior to the steady turbulent boundary layer theory establishing itself.

The flat plate theoretical solution derived for the computer used the ambient conditions and calculated shock speed and the normal shock relations to determine the flow conditions following the shock. The computer program prompted

the user for the ambient temperature and pressure and the Mach number of the flow. The time of transition between laminar and turbulent flow conditions was taken from the oscilloscope trace of the temeperature history of the flow. The program then solved Eqns. (1), (2), and (6) through (9) for the heat transfer rates using the unsteady heat transfer coefficient calculation. The theoretical and the experimental heat transfer rates corresponding to a given incident shock strength were plotted on the same graph. These plots are presented as figures 10 through 19.

The figures represent a heat transfer vs. time history at 2 inches (5.08 cm) from the leading edge of the plate for a range of shock Mach numbers from 1.09 to 1.32. Each figure shows the heat transfer corresponding to the laminar boundary layer development on the flat plate after passage of the shock wave. The high heat transfer rate that results from the initial flow of hot gas over the surface may be seen in the experimental data followed by its reduction as the laminar boundary layer develops. The theoretical heat transfer for laminar flow predicted by Eqn. (8) is shown for comparison. Dependent on the shock strength and flow conditions, the laminar heat transfer development attained quasi steady state by the time transition initiated, indicated by a large increase in heat transfer. After transition, the turbulent flow heat transfer predicted by Eqn. (9) is shown for

AMBIENT TEMP = 76°  
 PRESS= 29.1 IN/HG  
 MACH NUMBER = 1.095  
 TO NO. = F0502JU

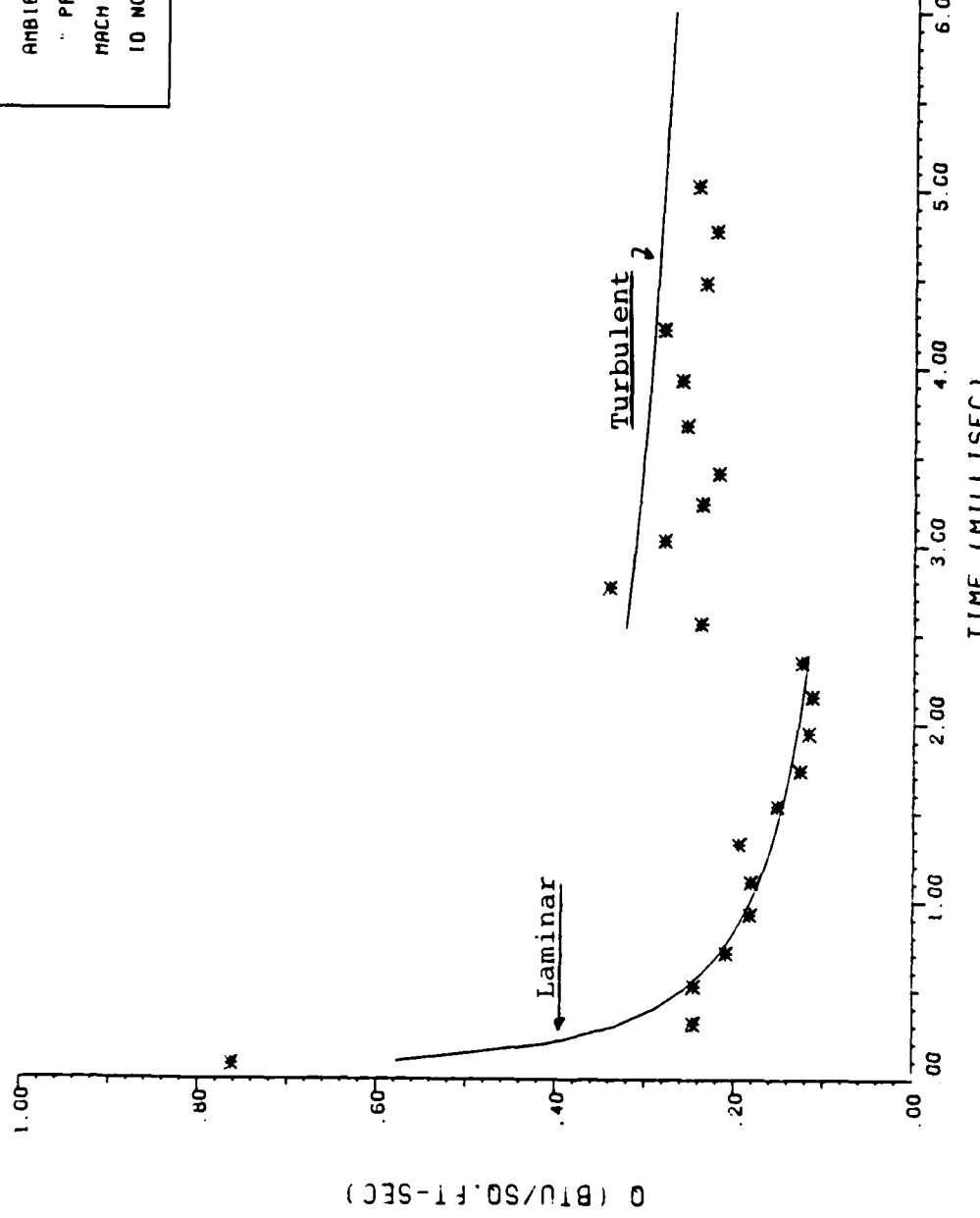


Figure 10: Flat Plate Heat Transfer ( $U_{\infty}=172$ fps)

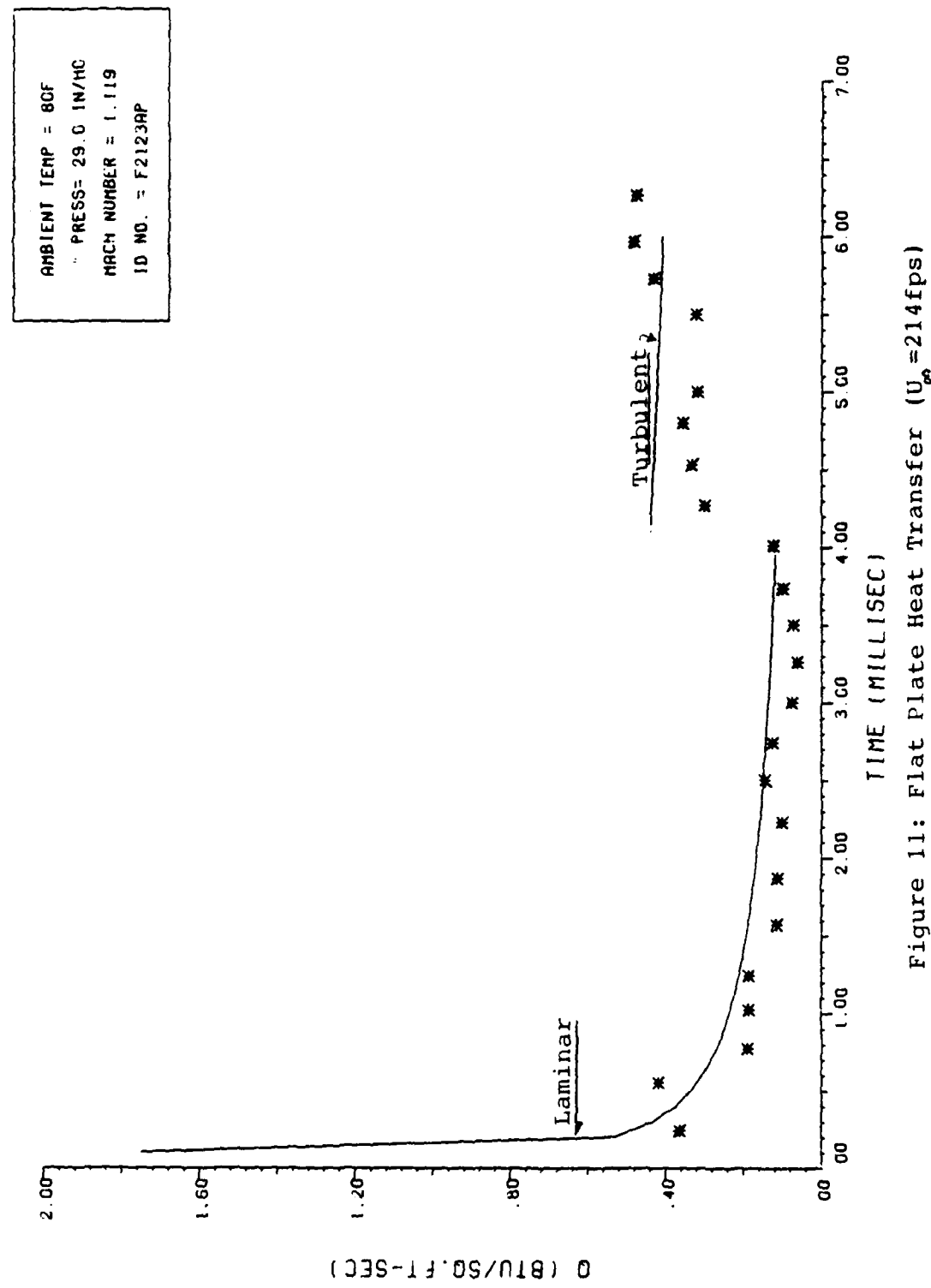


Figure 11: Flat Plate Heat Transfer ( $U_{\infty} = 214$  fps)

AMBIENT TEMP = 76°  
 " PRESS= 29.1 IN/HG  
 MACH NUMBER = 1.12  
 ID NO. = FC102JU

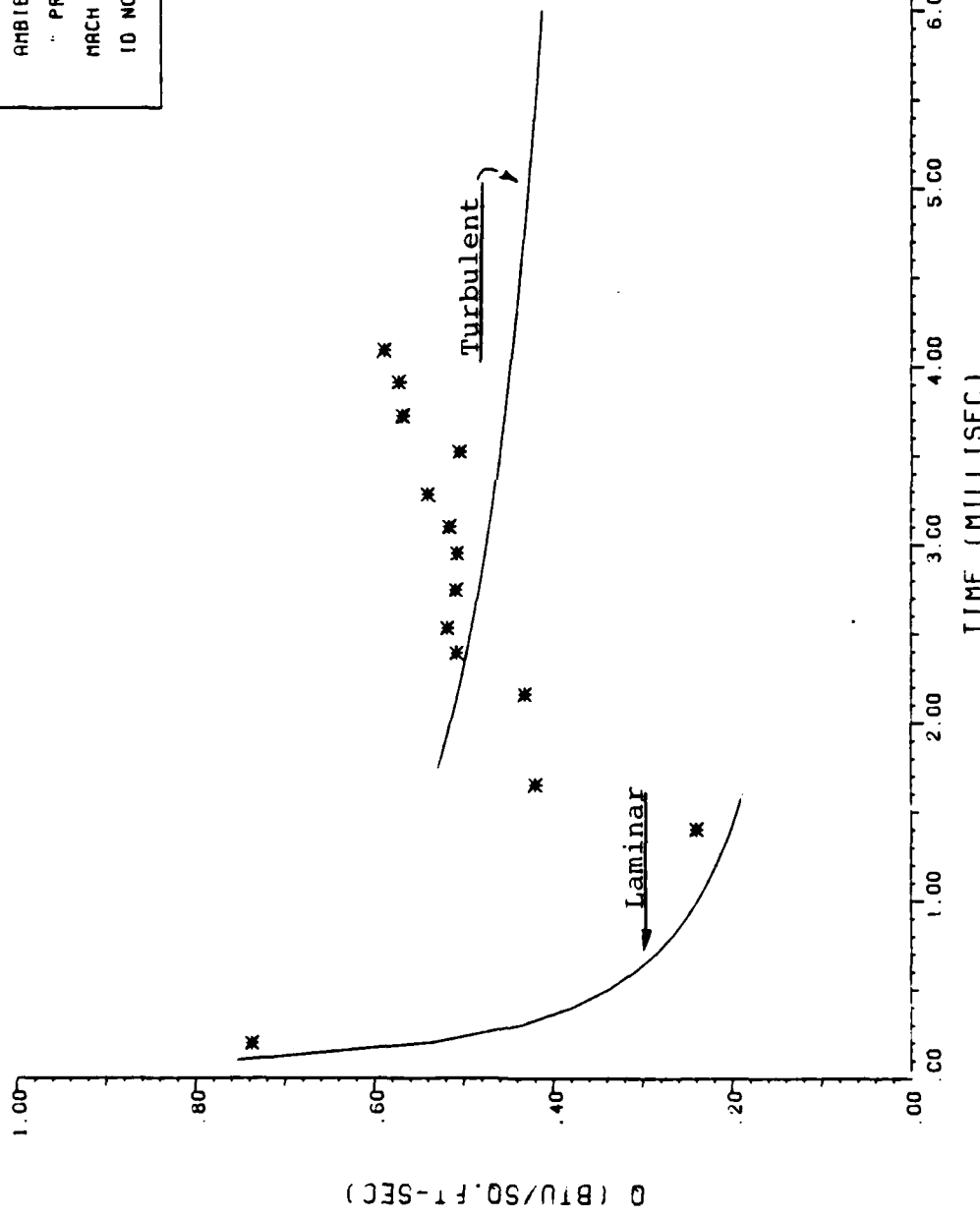


Figure 12: Flat Plate Heat Transfer ( $U_a=216$ fps)

AMBIENT TEMP = 76f  
 " PRESS=29.28 IN/HG  
 MACH NUMBER = 1.12  
 ID NO. = F0119A1

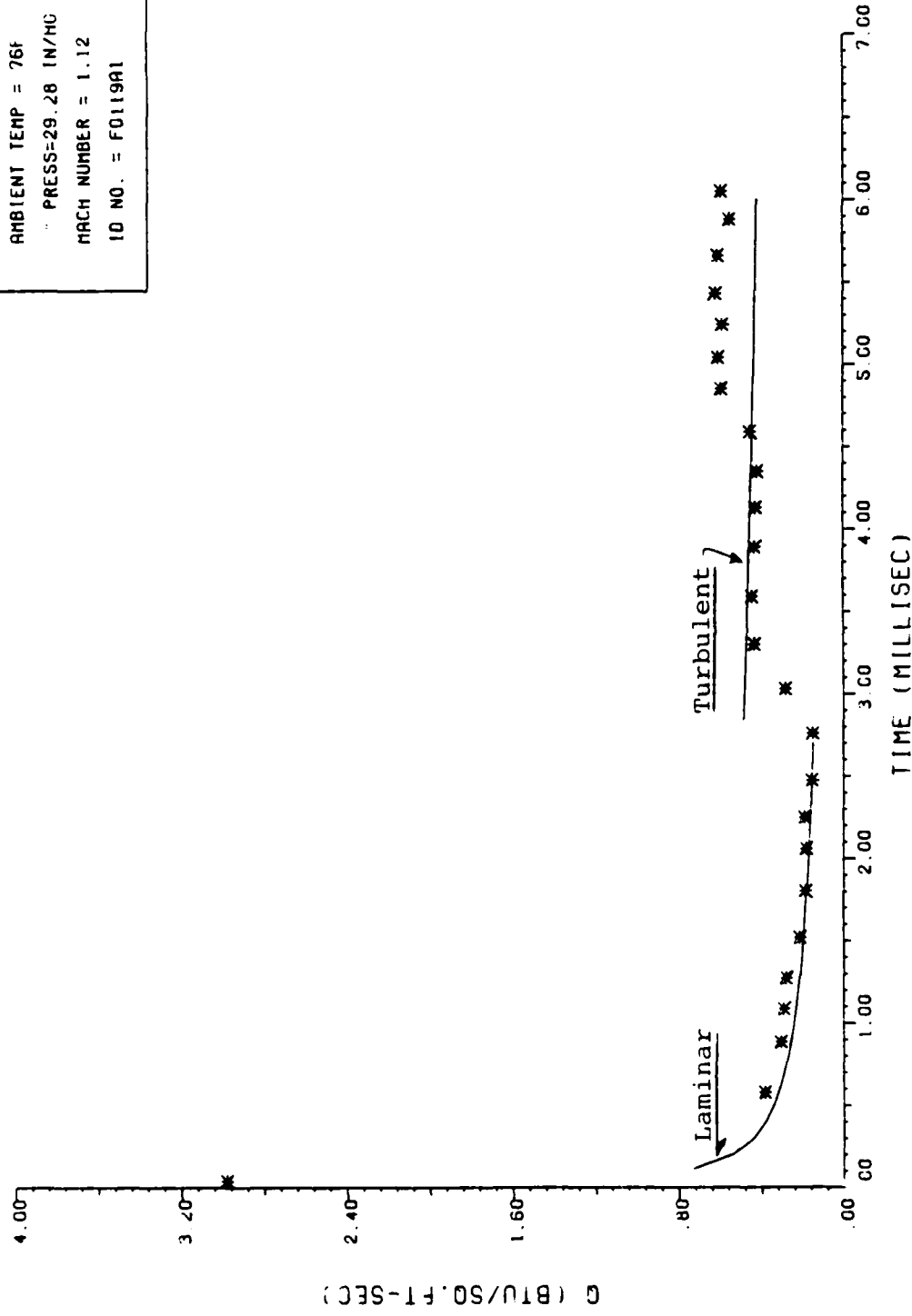


Figure 13: Flat Plate Heat Transfer ( $U_\infty = 216 \text{ fps}$ )

AMBIENT TEMP = 76°  
 " PRESS=29.28 IN/HU  
 MACH NUMBER = 1.162  
 ID NO. = F0219A1

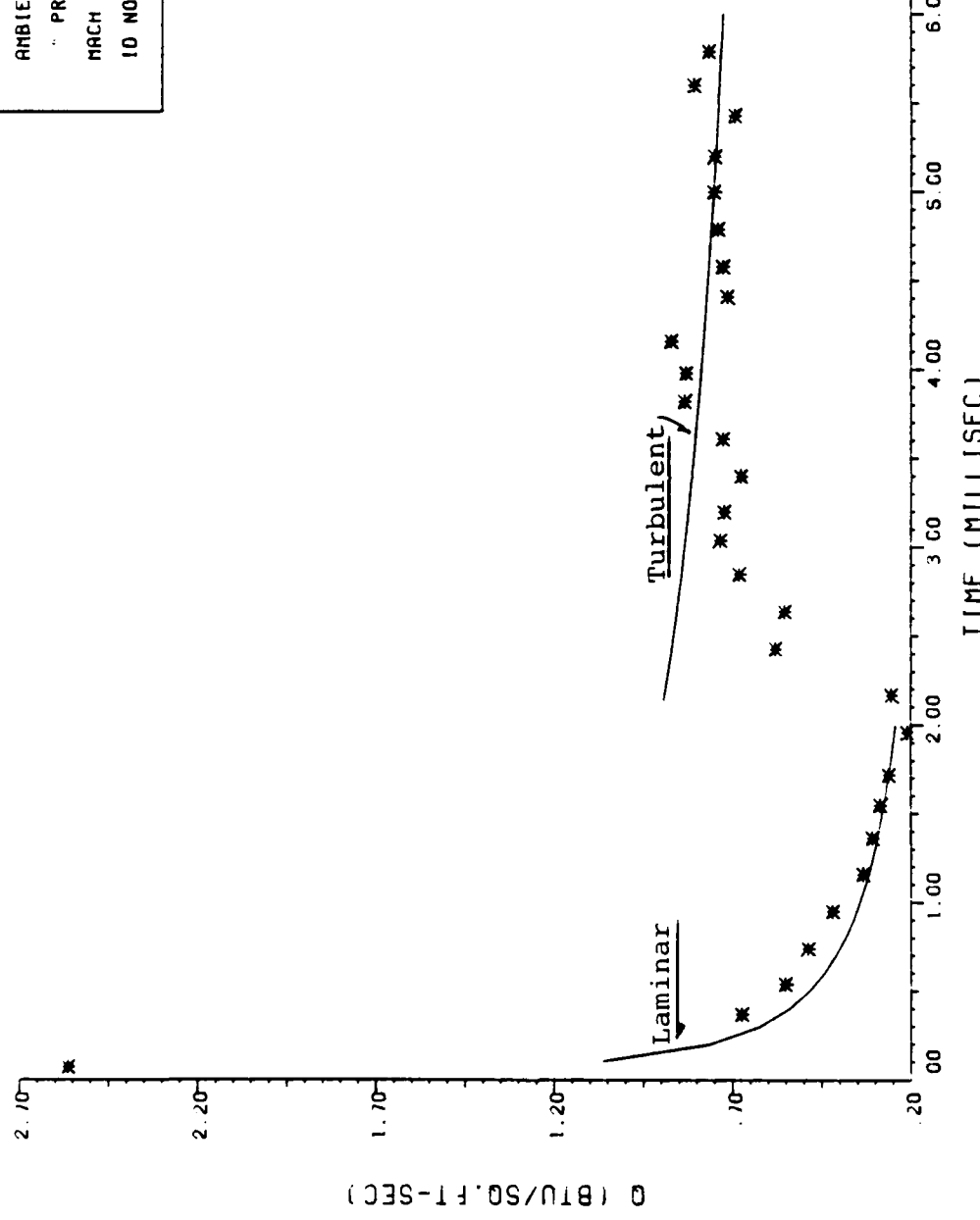


Figure 14: Flat Plate Heat Transfer ( $U_{\infty} = 284 \text{ fps}$ )

AMBIENT TEMP = 80F  
 PRESS=29.08 IN/HG  
 MACH NUMBER = 1.2367  
 ID NO. = F1823RP

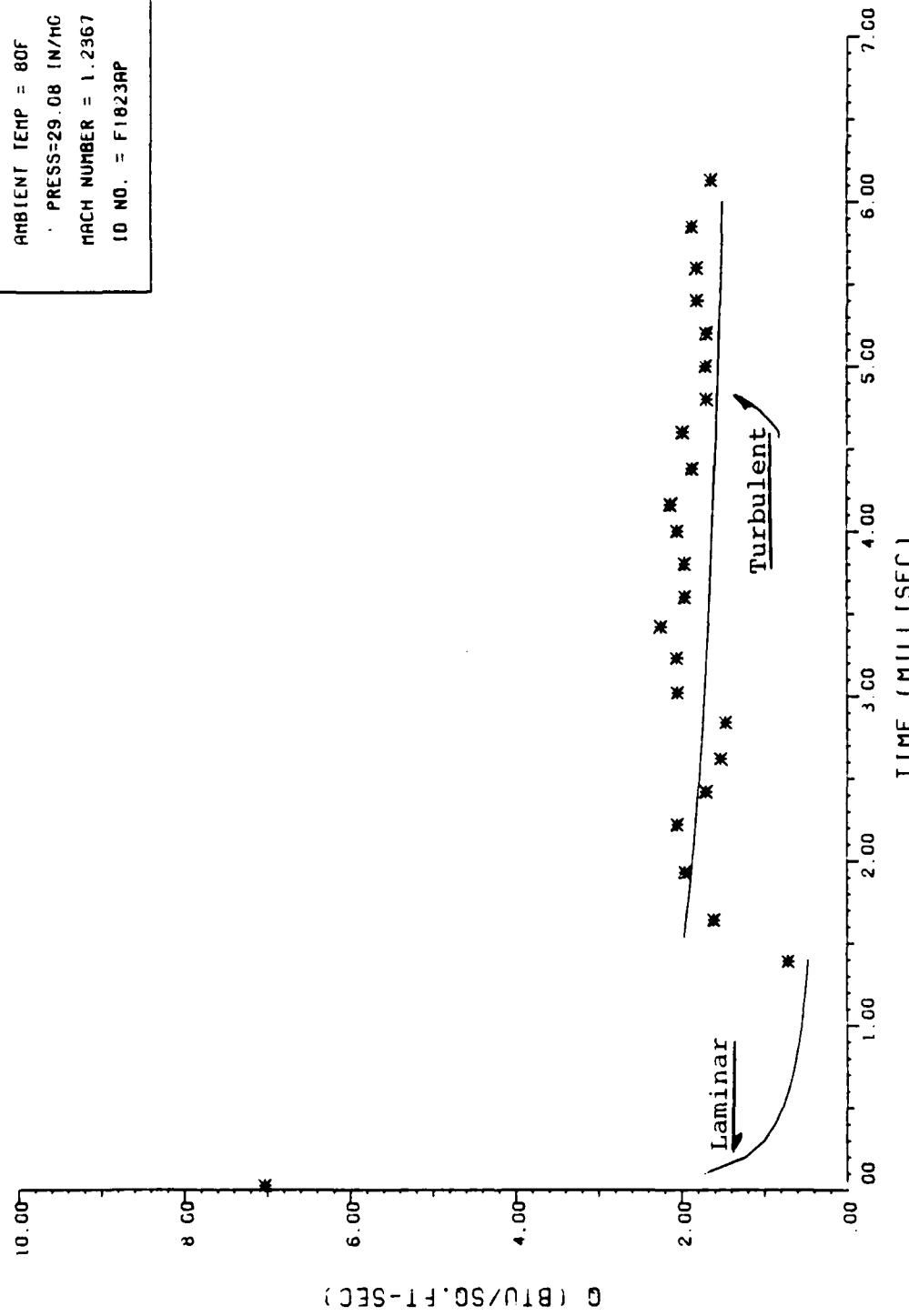


Figure 15: Flat Plate Heat Transfer ( $V_\infty=407$  fps)

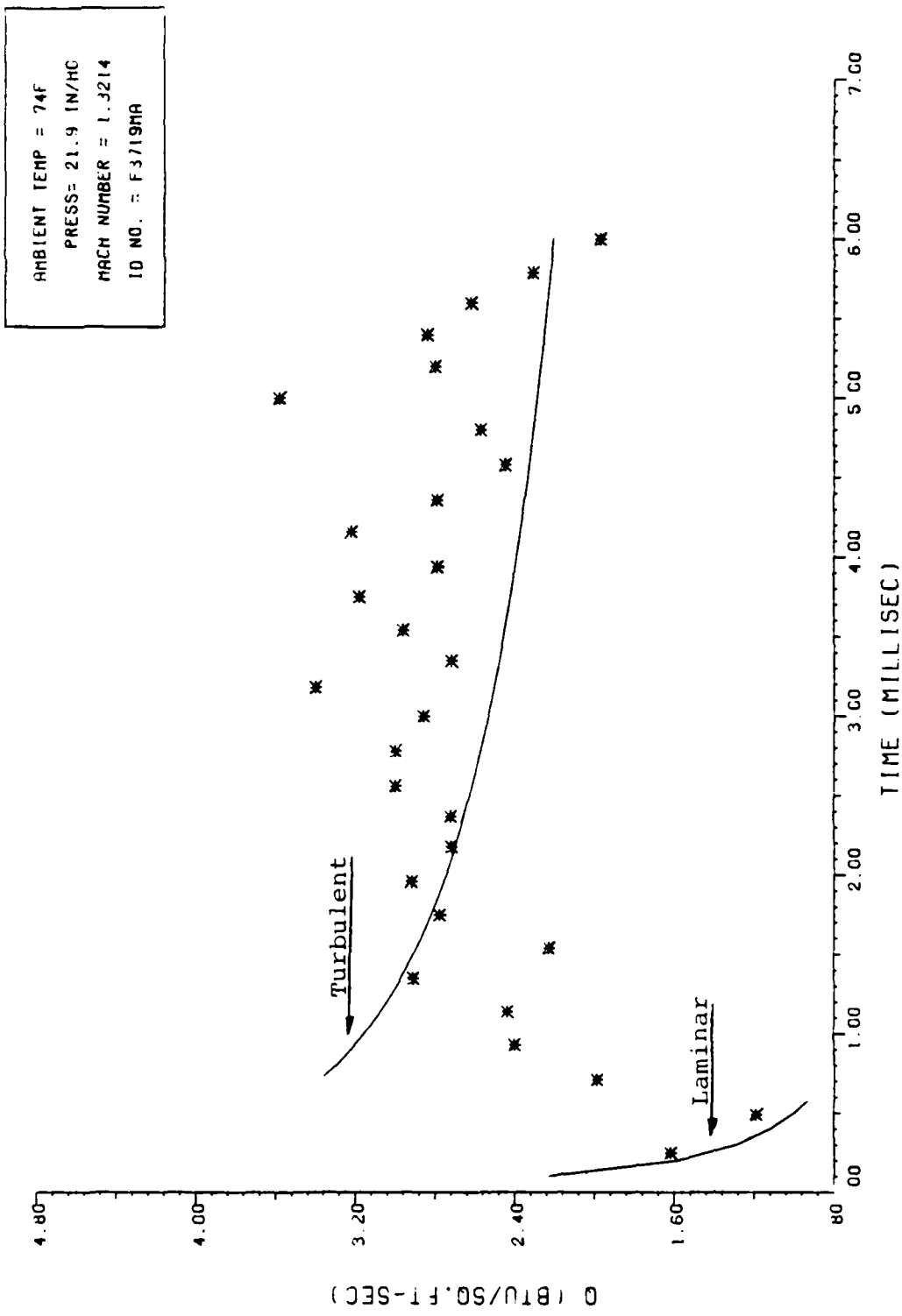


Figure 16: Flat Plate Heat Transfer ( $U_{\infty} = 536 \text{ fps}$ )

AMBIENT TEMP = 80F  
 PRESS=29.08 IN/HG  
 MACH NUMBER = 1.202  
 ID NO. = F1923AQ

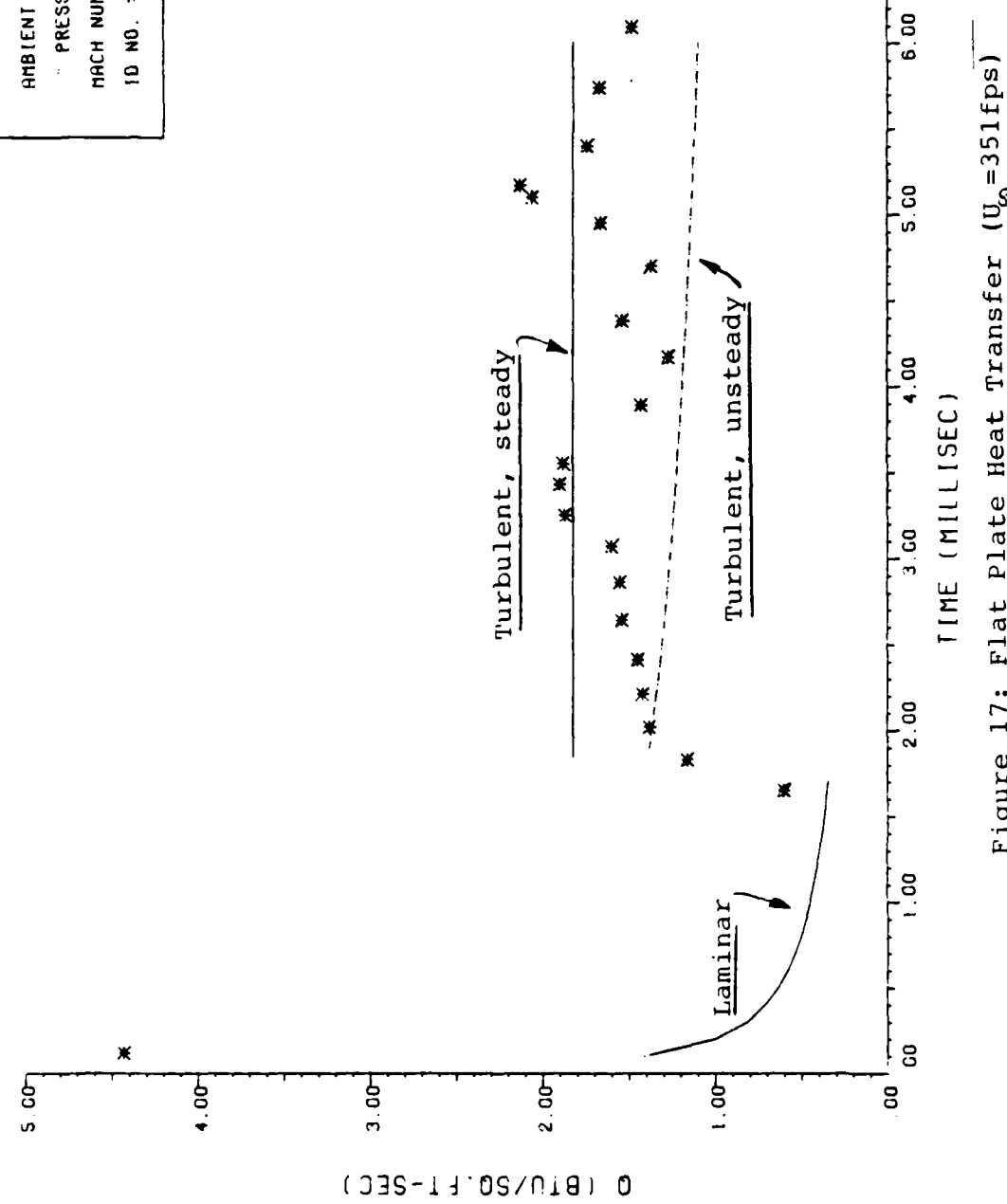


Figure 17: Flat Plate Heat Transfer ( $U_{Co} = 351 \text{ fps}$ )

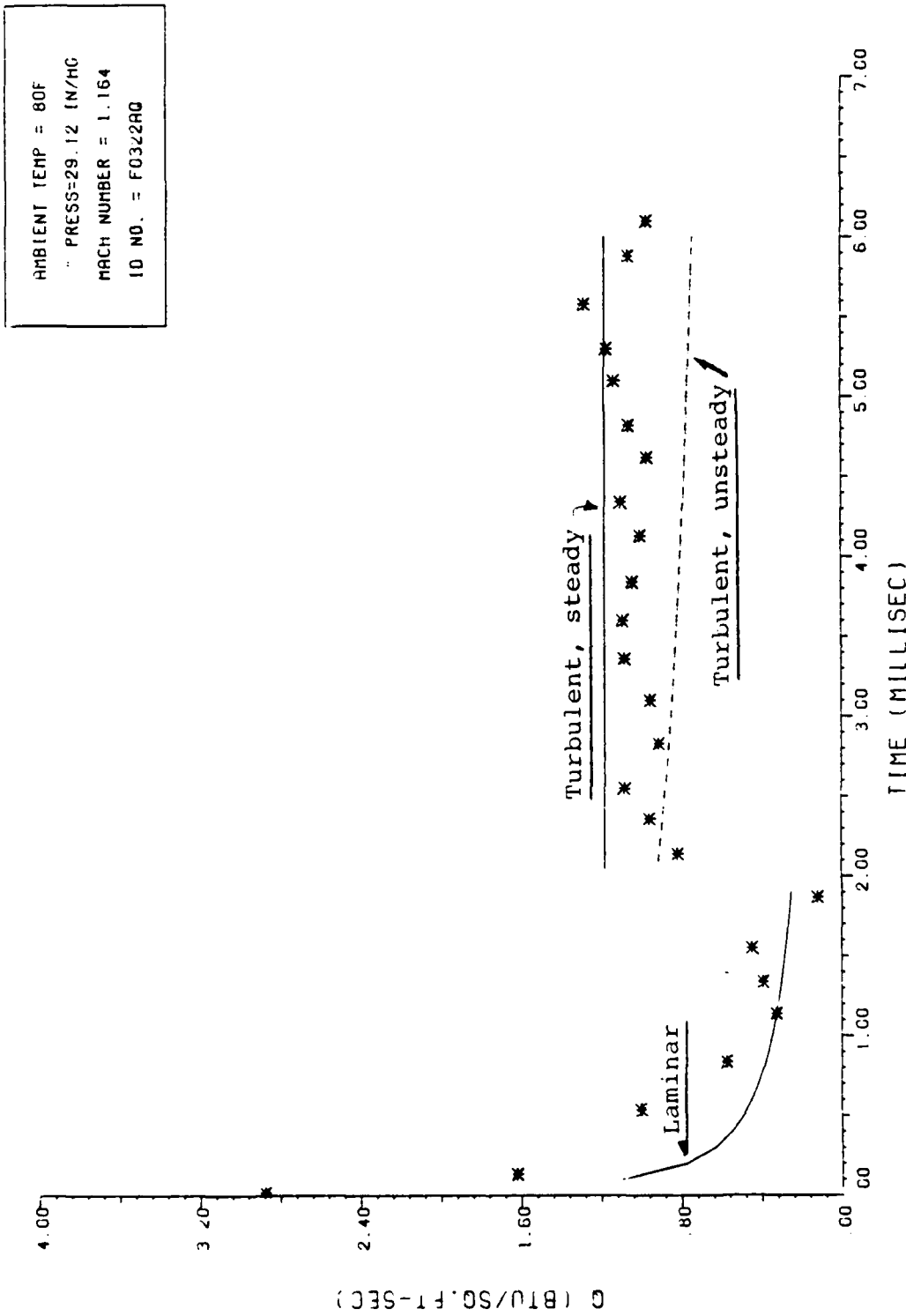


Figure 18: Flat Plate Heat Transfer ( $U_m = 289$  fps)

AMBIENT TEMP = 80F
PRESS=29.08 IN/HG
MACH NUMBER = 1.268
ID NO. = F1723A0

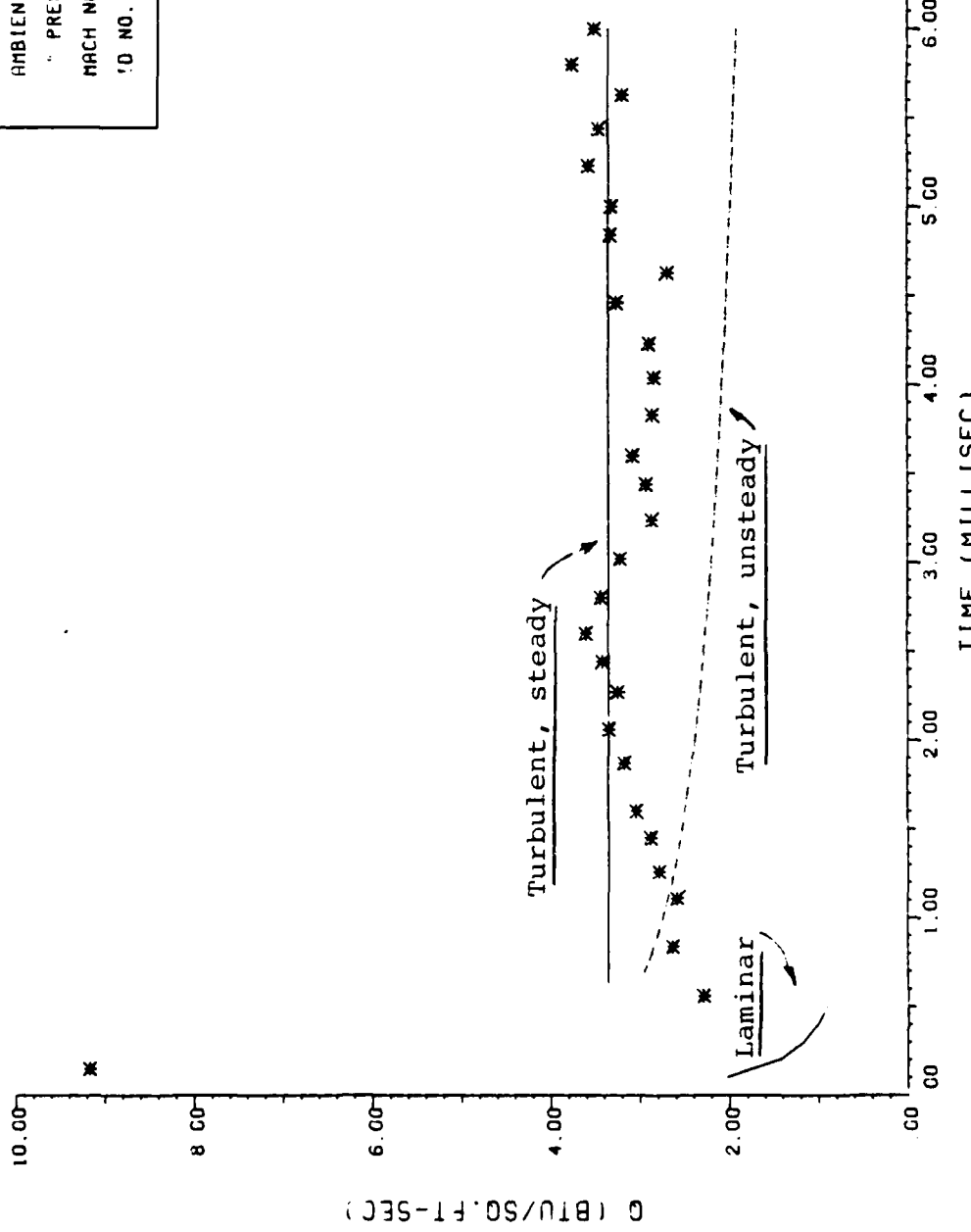


Figure 19: Flat Plate Heat Transfer ( $U_{\infty} = 470 \text{ fpm}$ )

comparison with the experimental data.

The figures show good agreement between laminar and turbulent heat flux measurements and theory. Examining only the laminar portion of the figures first, an error analysis indicated that the experimental data was within 37% of the theoretical curve at the worst correlation. Most of the experimental data fell within 10% of the theoretical curve. A possible explanation for this error was that when digitizing the photographic trace of the flat plate run, error arose due to inaccuracy in following the trace with the digitizer pattern. Approximating the true trace from the wide photographic trace could have lead to slight deviations. Many of the runs were digitized more than once to insure repeatability and accurate data reduction from the photographic trace, thereby minimizing this error. Also, for the numerical data reduction scheme to hold, the data needed to be digitized as close to a piecewise linear function as possible. Figures 10, 11, 13, and 14 show excellent agreement between theory and experiment. Deviation from the theoretical curves arose when the experimental laminar data was sparsely digitized as in figures 12 and 18. Accounting for these two possible sources of error would indicate that the laminar experimental data curves were in excellent agreement with the corresponding theoretical curves for the tested Mach number range.

Davies and Berstein (1969) indicated the laminar boundary layer with zero pressure gradient is substantially steady at a distance  $x$  from the leading edge of the plate after a time  $t$  given by

$$t = x / 0.3 * U_{\infty}$$

where  $t$  is measured from the instant of shock arrival at  $x=0$ , and  $U_{\infty}$  is the gas flow velocity. Figures 13, 14, 15, 17, and 18 satisfy this condition, i.e. steady laminar heat transfer was achieved. The Reynolds number in this regime was approaching a critical value when transition was initiated.

Analyzing the turbulent portion of the curves, the first noticeable difference was that the transition from laminar to turbulent heat flux measurements tended to be more gradual than the theoretical curves indicated. This confirms what Schlichting (1979) says is a transition region lasting for an undetermined time. The theoretical curves do not take into account the transition region but only predicted laminar heat transfer followed by that for turbulent flow. Evidence of transition is shown by the more gradual rise of experimental data after the minimum reached with laminar flow. Little work has been done to model the transition region for flow over a flat plate. For better agreement of experimental data in the future, an analytical solution should be derived and fitted into the present scheme taking into account the time for transition.

Part of the experimental turbulent data in figures 13, 14, 15, 17 and 19 agrees with the theoretical curves within a few percent. However, all the figures show data which was both lower and higher than the theoretical curves. Several explanations for these discrepancies are possible. The two aforementioned reasons for the laminar data could also hold true when examining the turbulent data. Free stream turbulence is another explanation for the high data points within some of the figures. These turbulence effects can be remarkably high with a turbulence intensity of about 2.5% producing an increase in heat flux on the order of 80% (Schlichting, 1979). This was evident in figures 12 and 14 at 3.5 ms and in figure 16 where it was scattered throughout. In figures 17, 18 and 19, there are two theoretical turbulent curves per plot. The dashed line curve represented the turbulent theory based on a heat transfer coefficient derived from employing a non-steady Reynolds number calculated from the equation

$$Re_x = \frac{U_{\infty} x}{v}$$

where  $U_{\infty}$  is the gas flow velocity,  $t$  is the time the flow has instantly passed the leading edge, and  $v$  is the kinematic viscosity evaluated at the reference temperature. These curves are similar to figures 10 through 16. However, further investigation revealed that when the heat transfer coefficient was derived from a steady Reynolds number

calculation, given by

$$Re_x = U_\infty^* x / v$$

where  $x$  is a fixed position on the flat plate, the theory offered a better correlation with the experimental data. The solid curve indicated a maximum error of approximately 20% between theory and experimental data. As seen in figures 17, 18, and 19, noticeable improvement existed once the modification was done. This anomaly of the steady heat flux calculation fitting some of the experimental data better than the unsteady heat flux calculation indicates some criteria is influencing the development of the turbulent boundary. Whether the criteria be the roughness of the plate, or free stream turbulence, or Reynolds number momentum thickness, the criteria should be looked at in future shock tube work.

The agreement between the flat plate experimental data and the theoretical solution provides verification for both the experimental procedure and the finite difference routine used to reduce the data.

#### Turbine Vane Heat Transfer

The temperature histories from the six heat flux gages on the vanes were reduced through the proven flat plate numerical scheme into the heat flux history of figures 20 through 29. The data were plotted two different ways: first the heat transfer distribution along the vane suction side surface is plotted at a given Mach number; second, the heat transfer vs.

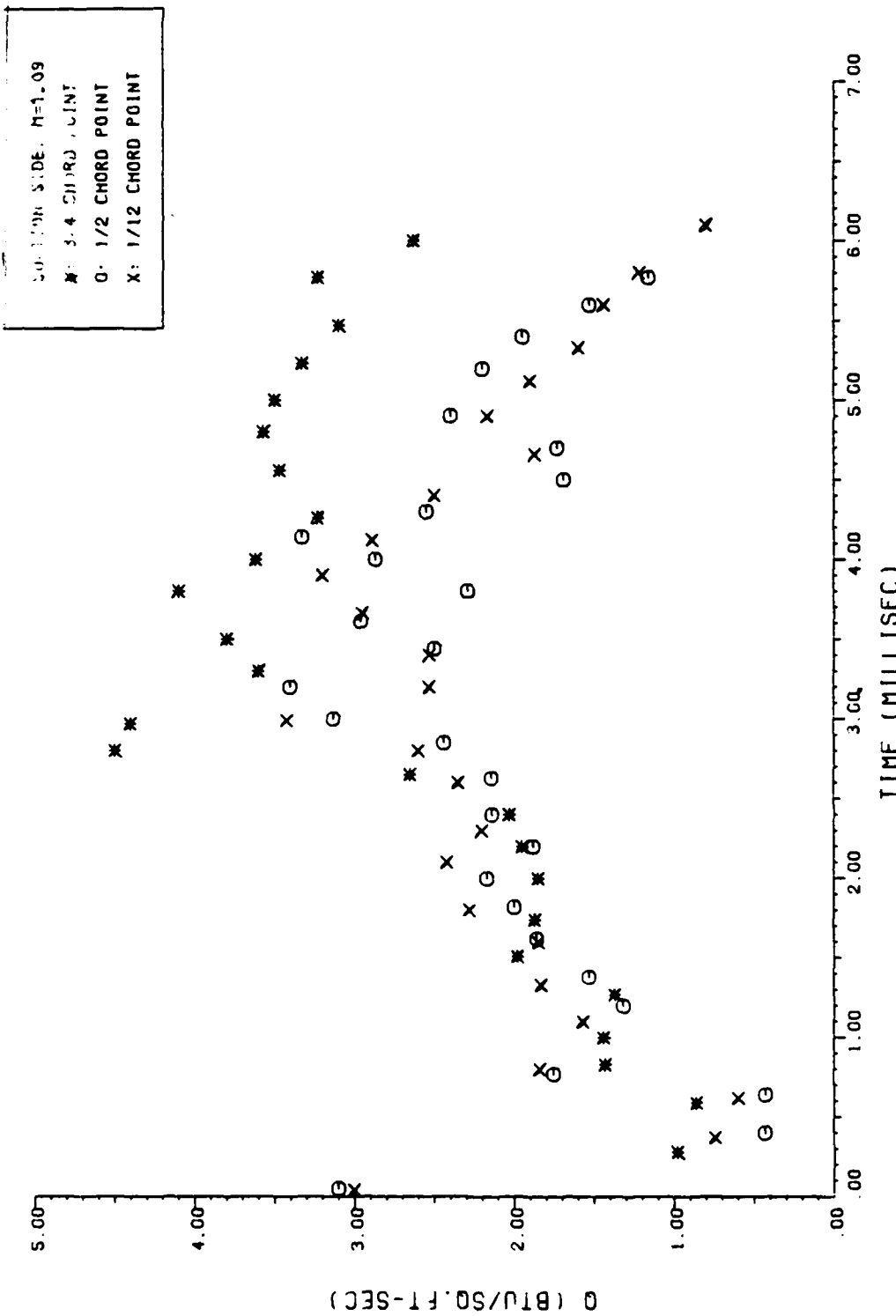


Figure 20: Turbine Vane Heat Transfer ( $U_{\text{avg}} = 164 \text{ fps}$ )

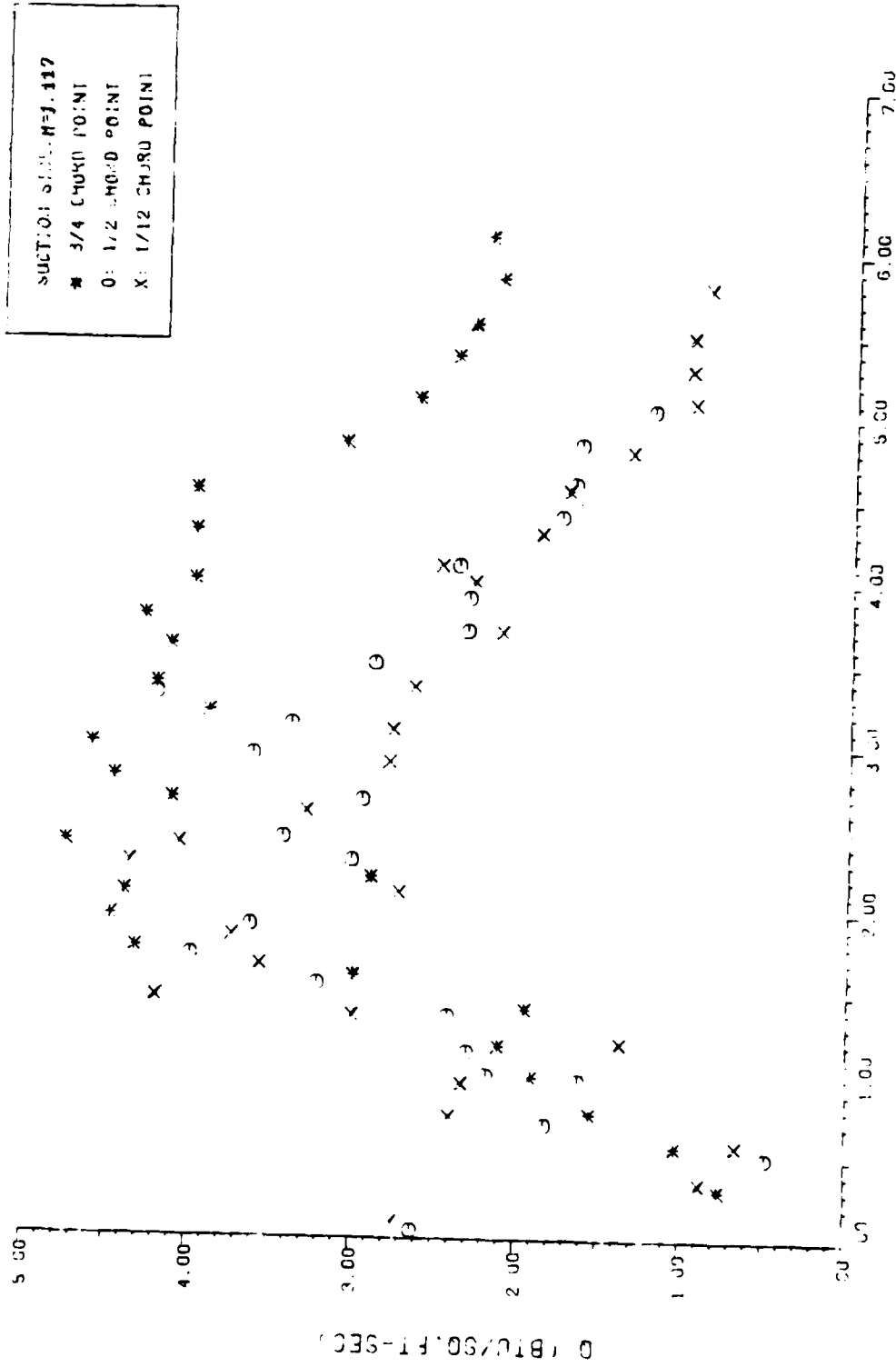


Figure 21: Turbine Vane Heat Transfer ( $U_n = 211 \text{ fpm}$ )

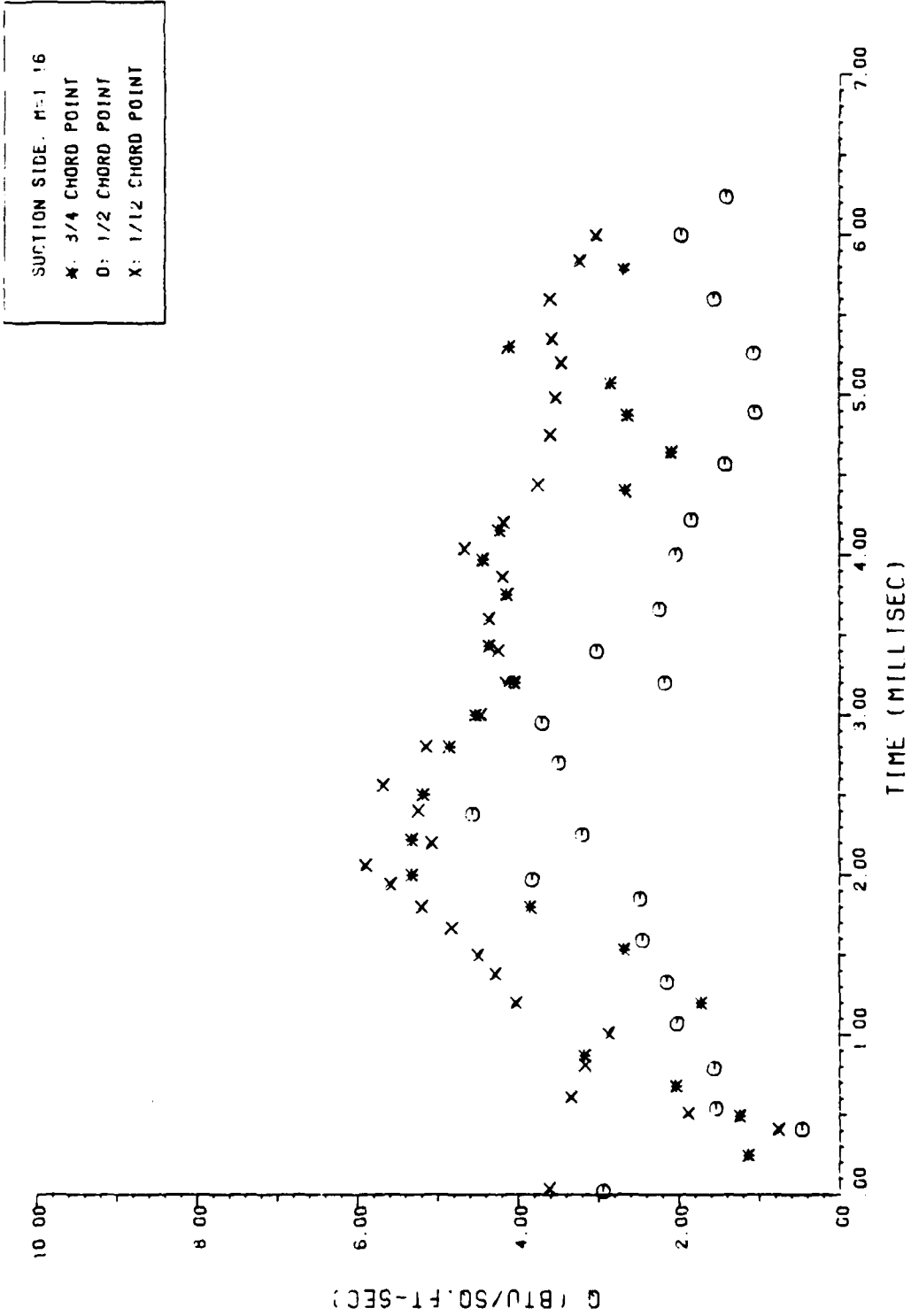


Figure 22: Turbine Vane Heat Transfer ( $U_{\infty} = 283 \text{ fps}$ )

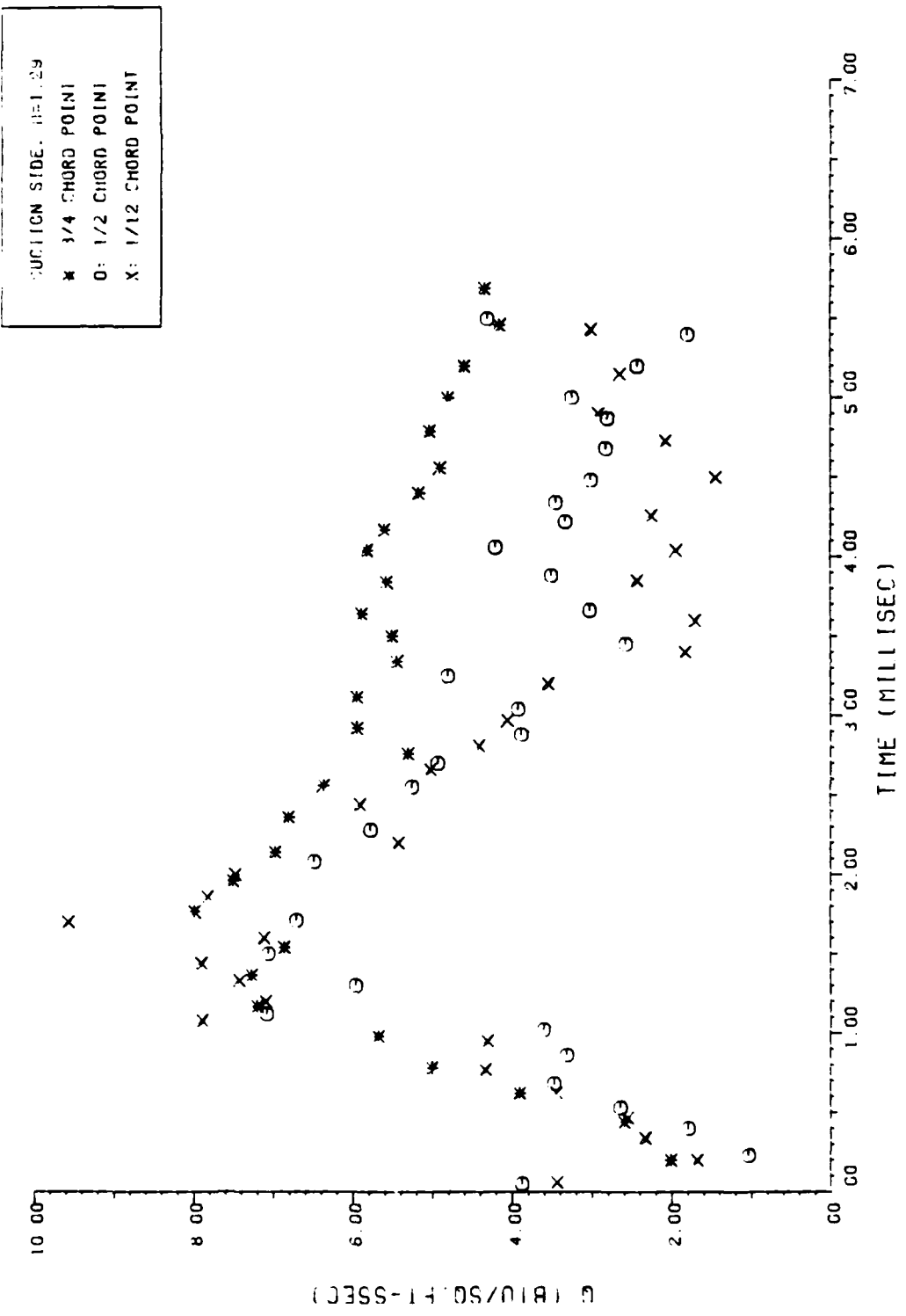


Figure 23: Turbine Vane Heat Transfer ( $U_{\infty} = 489 \text{ fps}$ )

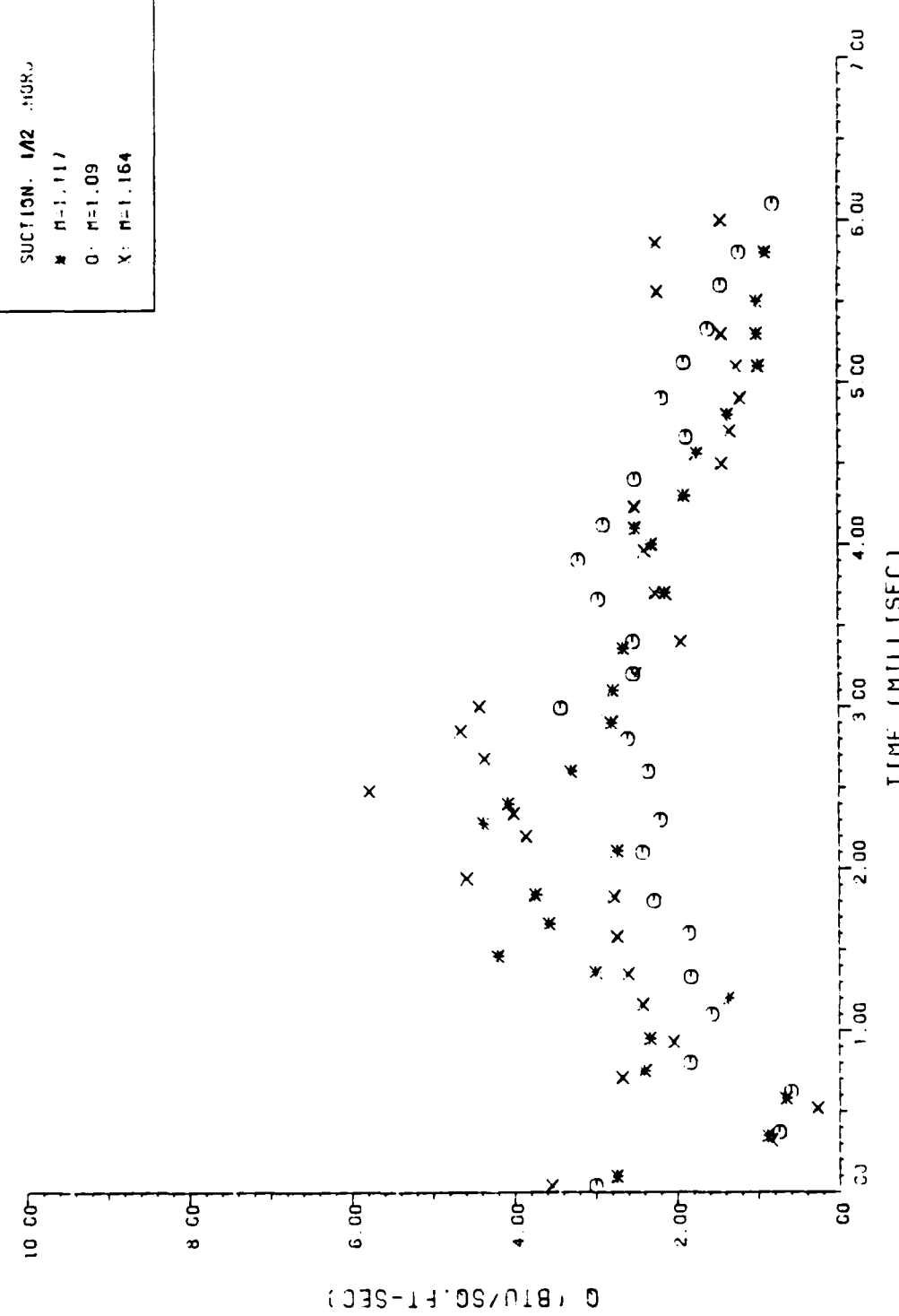


Figure 24: Turbine Vane 1/12 Chord Suction Side  
Heat Transfer

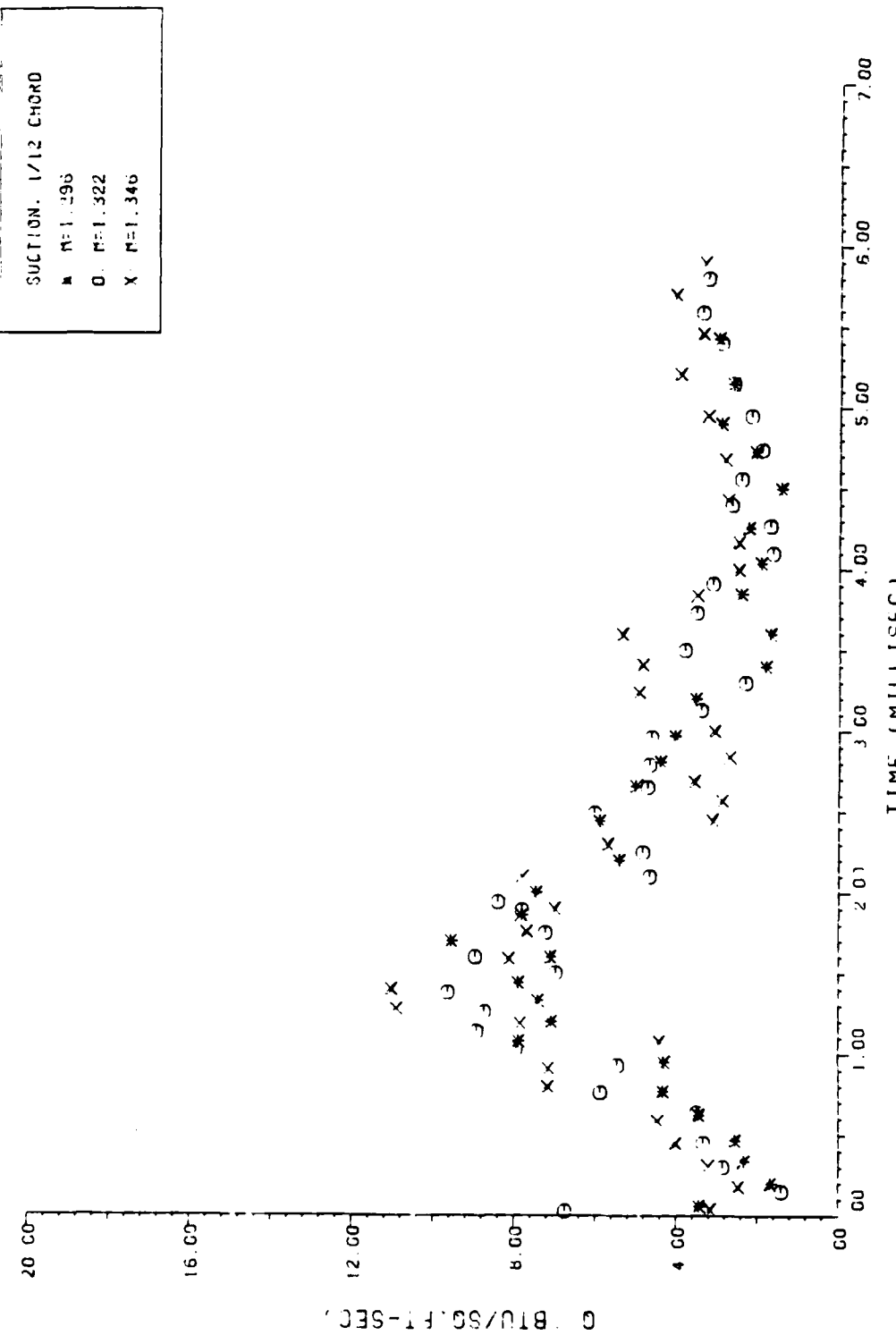


Figure 25: Turbine Vane 1/12 Chord Suction Side  
Heat Transfer

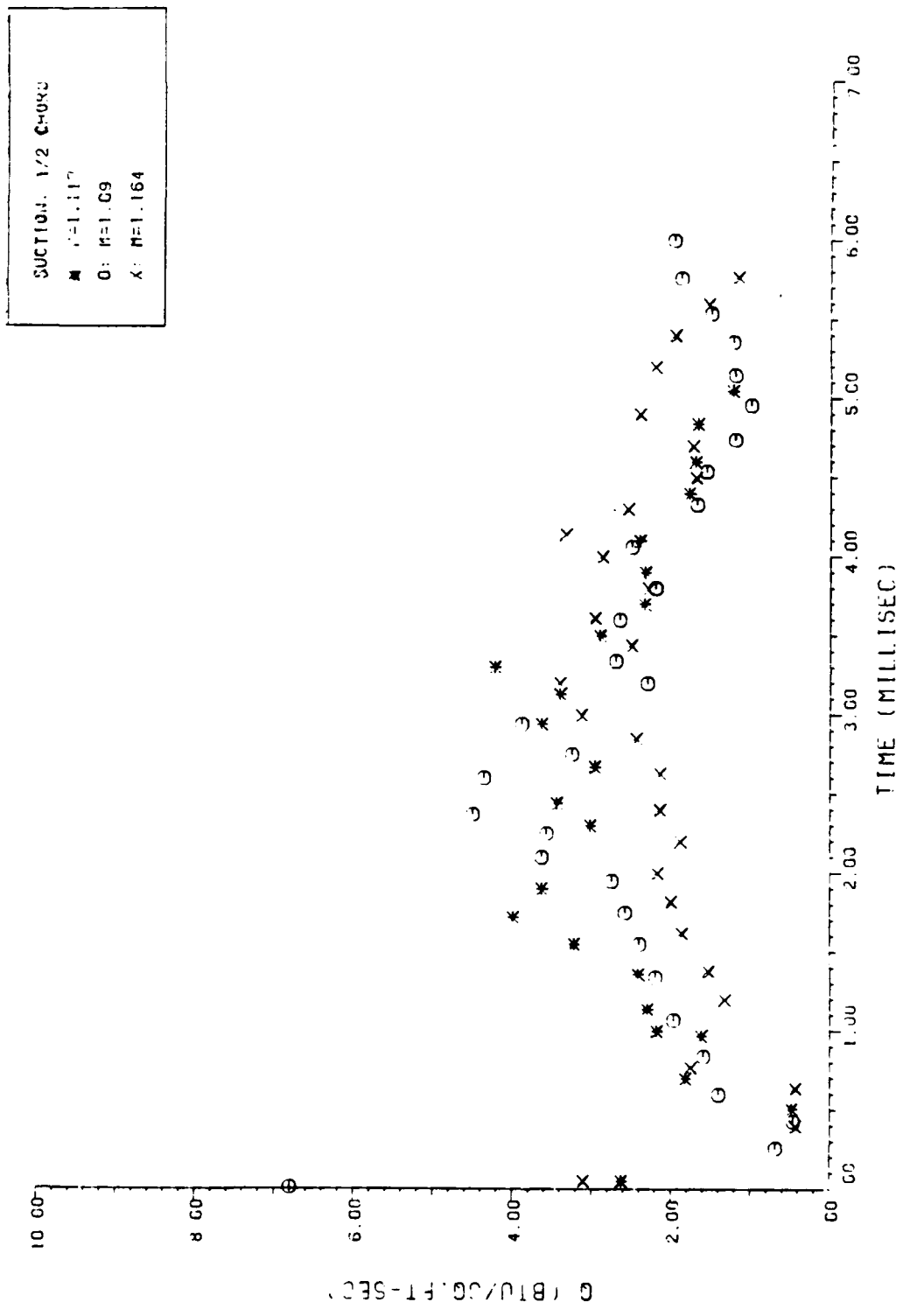


Figure 26: Turbine Vane 1/2 Chord Suction Side  
Heat Transfer

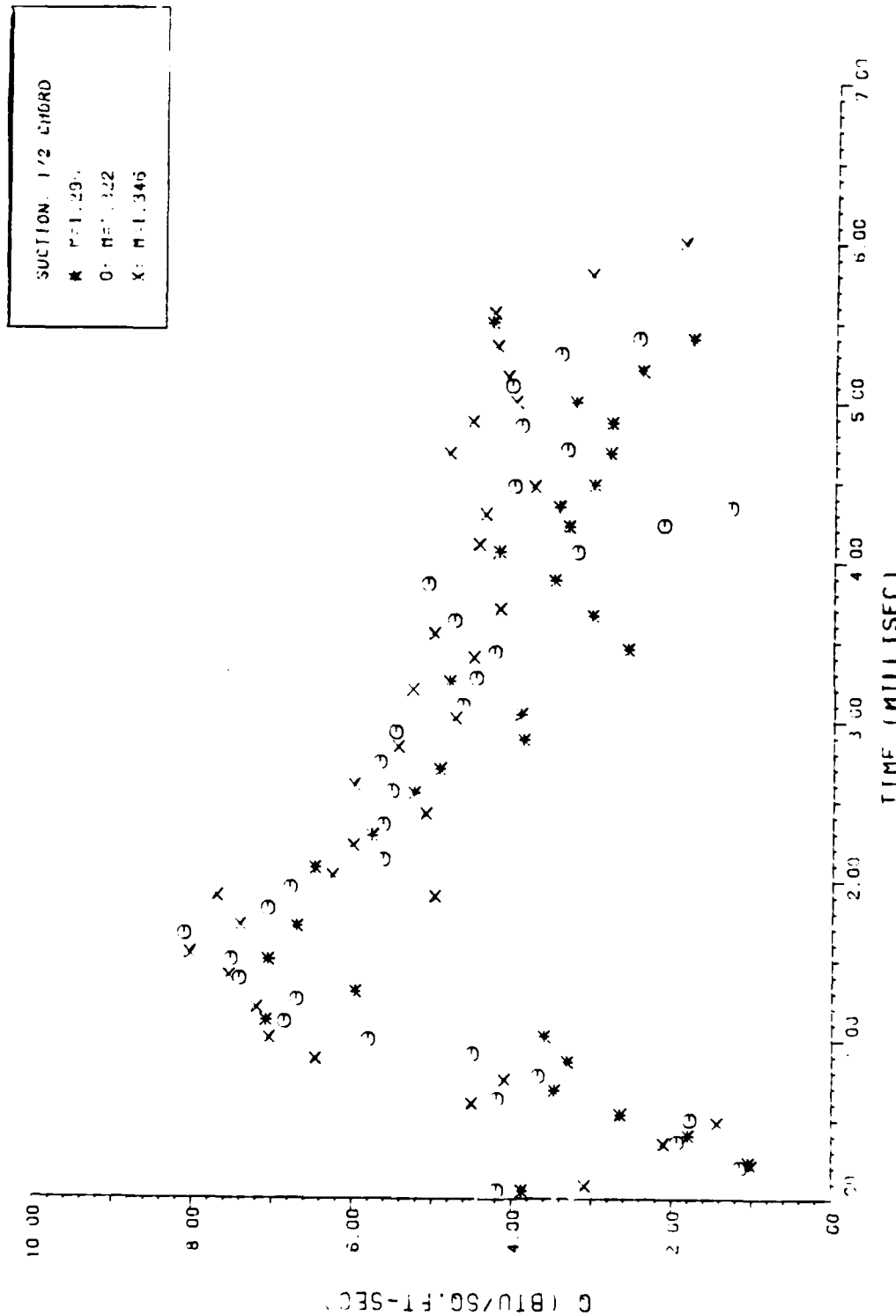


Figure 27: Turbine Vane 1/2 Chord Suction Side Heat Transfer

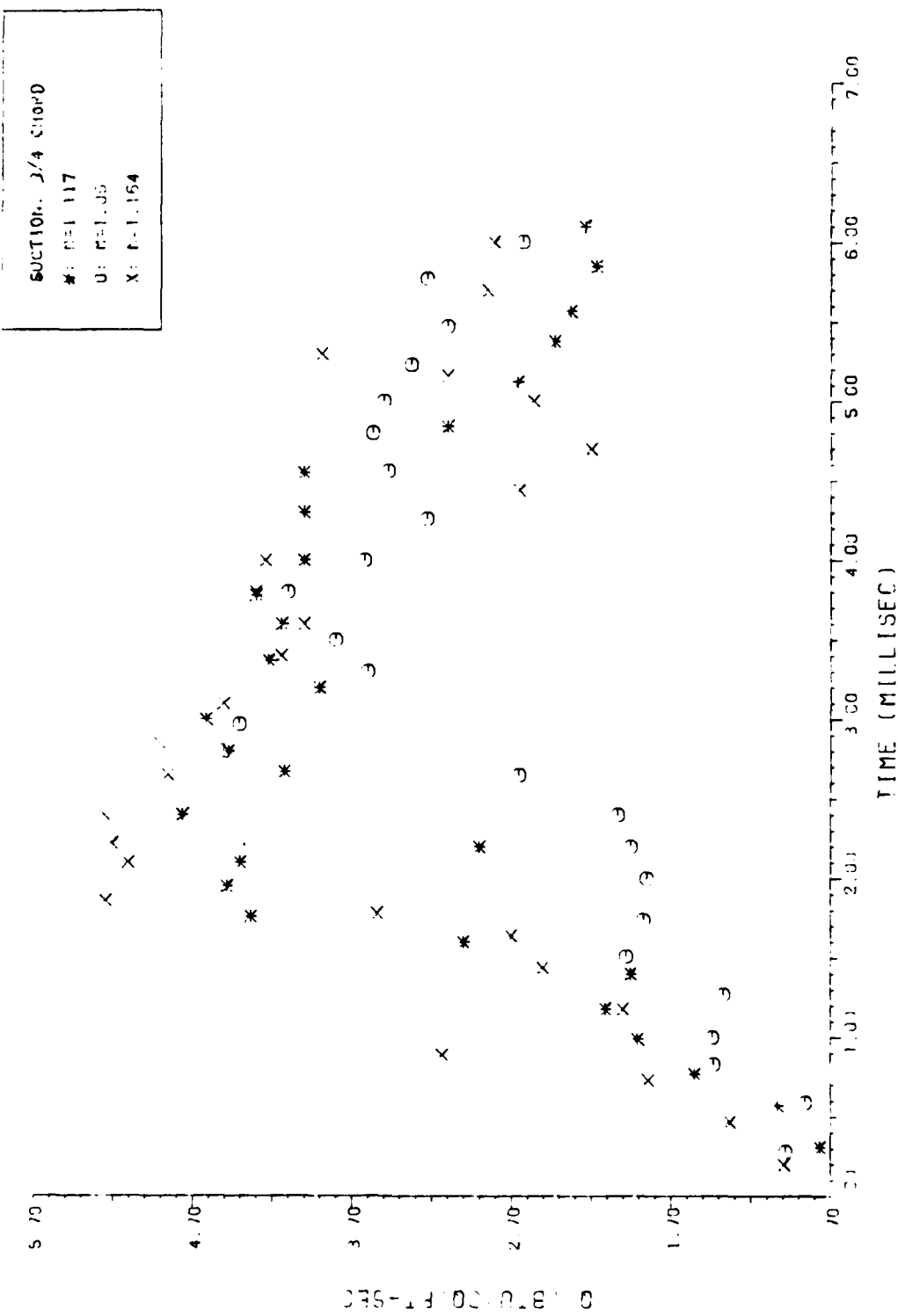


Figure 28: Turbine Vane 3/4 Suction Side Heat Transfer

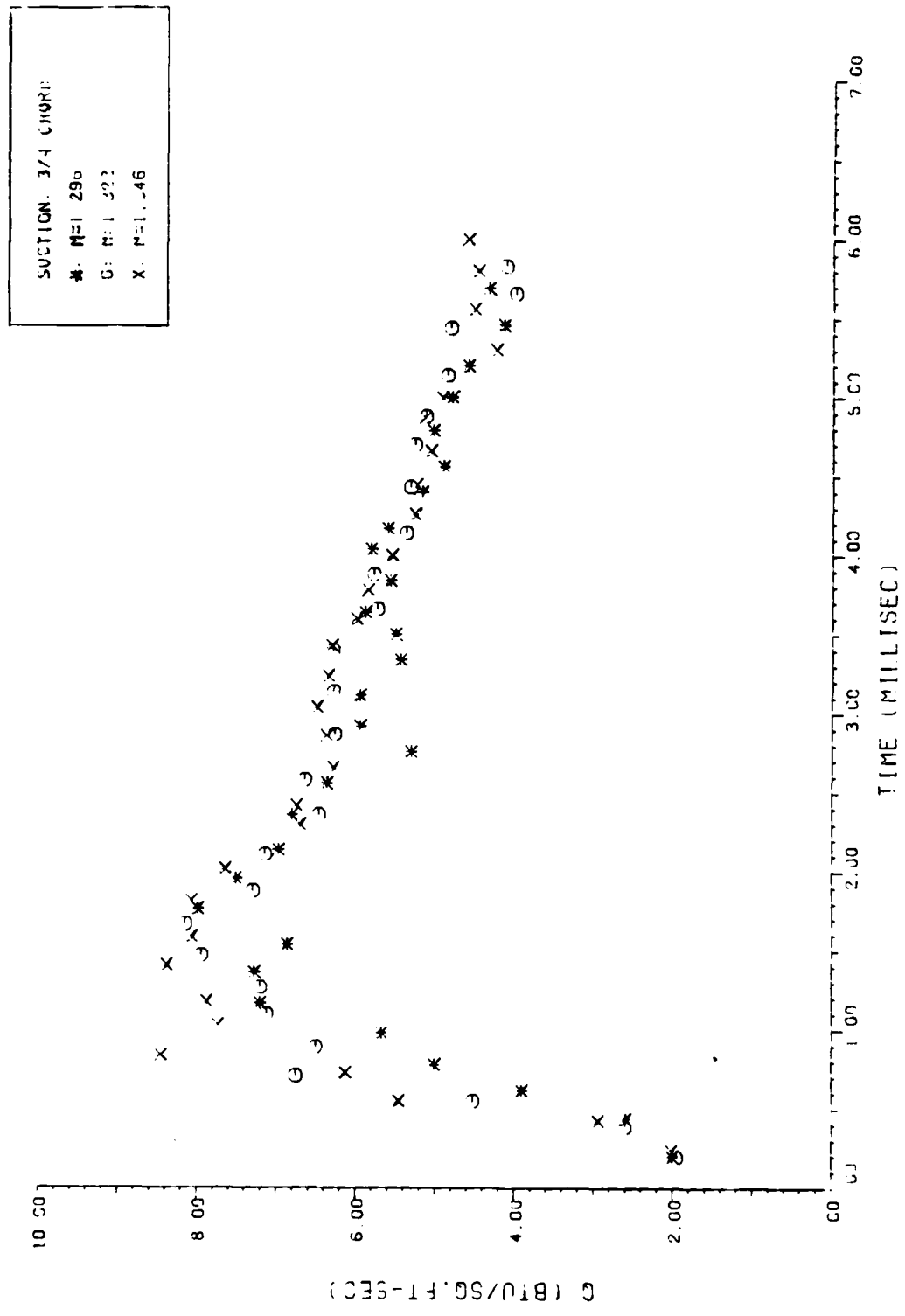


Figure 29: Turbine Vane 3/4 Chord Suction Side Heat Transfer

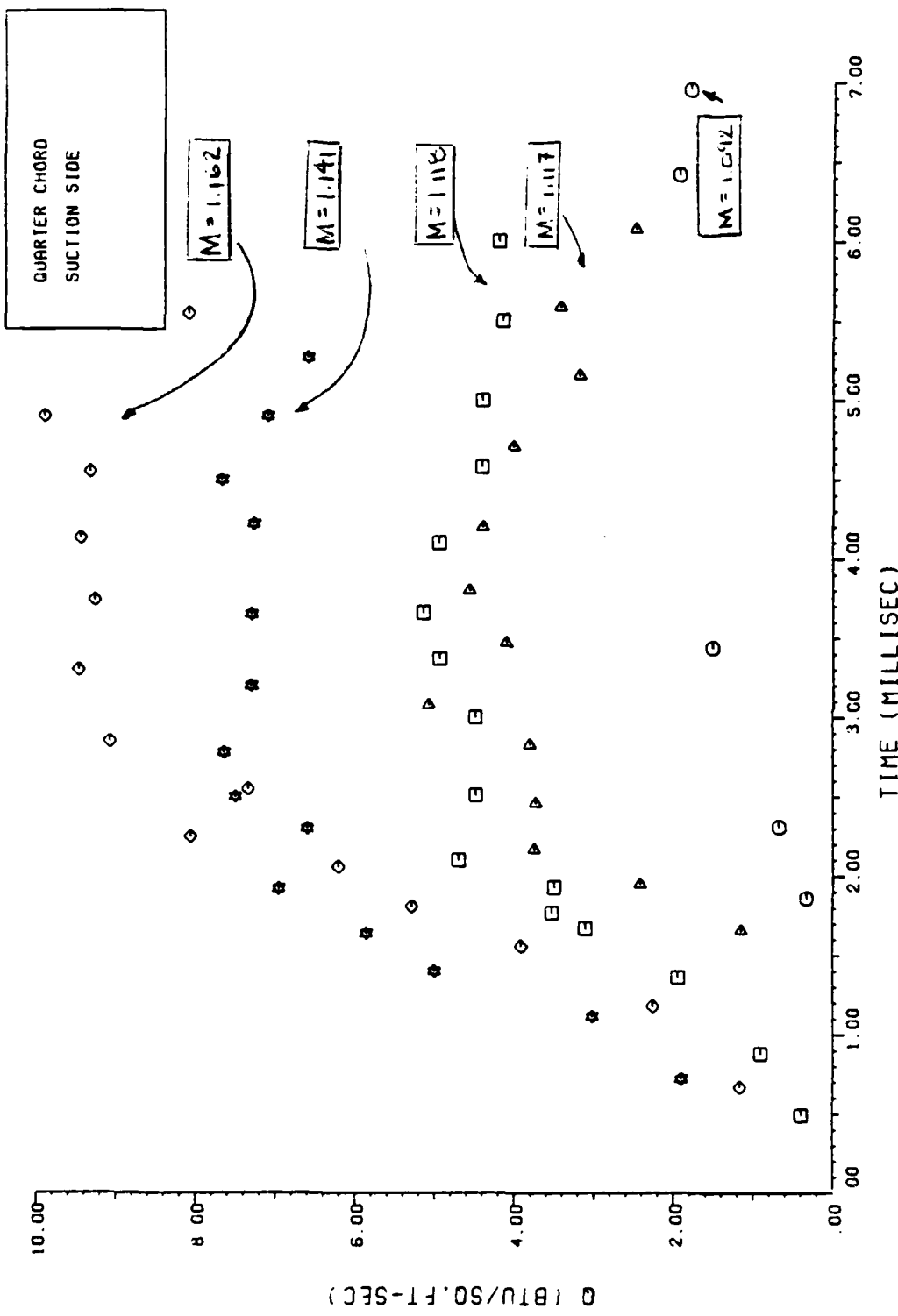


Figure 30: Turbine Vane 1/4 Chord Suction Side  
Heat Transfer

time history is plotted for one chord position on the vane surface.

Analyzing the figures, several observations can be made. At the 1/12 chord and 1/2 chord suction side, a step-rise in temperature resulting in a high heat transfer was recorded. Then both gages, independent of initial conditions established by the shock tube in the range investigated, experienced a transition at 0.5 milliseconds. This repeatable occurrence indicated that the transition, while independent of initial conditions, might be dependent on the turbine cascade geometry. Evidence of this transition has been documented through interferograms by Gochenaur (1984) who concluded that the suction side boundary layer was turbulent by the time it reached the 1/4 chord point. Gochenaur was using a thermocouple to record his heat transfer measurements. However, in figures 24 and 25, data for the 1/12 chord, and figures 26 and 27, data for the 1/2 chord, the plots indicate that there existed a short laminar startup then a rapid transition to turbulent flow. This is further supported by figures 28 and 29, data at the 3/4 chord, which show the data to be already transitioned to a non-laminar boundary layer. Gochenaur (1984) indicated that transition had occurred prior to the 1/4 chord position on the suction side. The present study indicates that the transition occurred not only prior to the 1/4 chord but prior to the 1/12 chord position. When

examining the test vane profile of figure 7, the 1/12 chord position on the suction side is about half way from the stagnation point of the vane to the 1/4 chord position along the vane surface. Thus, transition at the 1/12 chord point is possible since the position is a considerable distance around the vane surface.

When comparing a particular gage's heat flux history for different initial conditions, quasi steady state heat fluxes were not established until 2 milliseconds had elapsed from the initial shock reflection. The inlet and outlet pressure transducers also arrived at steady state after 2 milliseconds from flow startup. All gages showed a higher heat flux corresponding to higher initial temperature and pressure. At low initial conditions corresponding to shock tube shock strength of  $M=1.09$ , the data for the 1/12 chord and 1/2 chord show a gradual rise and decline in the slope, see figures 20, 24 and 26. Increasing the shock strength increased the slope of the data for both chord positions and it peaks at a higher heat flux in less time from flow initiation than at the low shock tube Mach number.

When analyzing the 3/4 chord position in figure 21, there is an initial rise in heat flux possibly indicating no laminar startup region at all. In addition the heat transfer values for the 3/4 chord are greater than at both 1/12 and 1/2 chord positions. This difference in heat transfer could be the

result of the flow geometry or the free stream turbulence effects. This trend in high heat transfer near the trailing edge would indicate that emphasis needs to be placed on cooling in this region.

For the low Mach number range, the 3/4 chord position attained a quasi steady-state which lasted longer than that for the 1/12 chord and 1/2 chord position as seen in figure 20. This phenomenon may also be seen in figures 22 and 23 at the higher shock strength. One possible explanation could be that a separation point near the 3/4 chord point existed. From figure 20, the 3/4 chord point indicated a separation region occurred at the 2.7 millisecond mark. This separation region enables a more rapid and thorough mixing of the turbulent boundary layer resulting in higher heat flux measurements. However, the heat transfer coefficient, based on  $x$  to the 1/5 power, would indicate a lower heat flux further out from the stagnation point ( $x=0$ ). With separation near the 3/4 chord point, an adverse pressure gradient might influence the heat transfer to be higher than expected. Preliminary data from the previously mentioned STAN 5 computer program indicates that a separation region may indeed be present near the 3/4 chord point of the turbine vane suction side (Stanek, 1985). Additionally, evidence of the higher than expected heat flux rate near the trailing edge was shown by a large displacement of fringes at the suction surface in the

finite fringe interferometer pictures by Gochenaur (1984). The large shift in the fringes is indicative of a large density gradient which corresponds to a high heat flux. Another possible effect contributing to the increased heat flux rate might be the contribution of the free stream turbulence. As mentioned before in the flat plate analysis, turbulence effects can be remarkably high with a turbulence intensity of about 2.5% producing an increase in heat flux on the order of 80% (Schlichting, 1979). Further studies correlating experimental data with the STAN 5 predictions should be accomplished.

The pressure side data were not included because of the time required to adequately digitize and analyze the suction side data. However, the pressure side data are available for future study.

#### Flow Visualization

Some excellent photography was made indicating the laminar boundary layer growing and transitioning into a turbulent boundary layer. Figure 30 (a) through (d) shows the history for different shock runs at equal shock strength. The flow travels from left to right. The pictures differ in a delay trigger count of approximately 0.3 milliseconds. Figure 30 (a) shows a thin white line along the top of the flat plate with the thermocouple lead extending from the plate to the right. This thin white line is indicative of a laminar

boundary layer lying on the surface. As the flow travels downstream, the white line thickens with time, as pictured in figure 30 (b). In figure 30 (c) a transition is beginning to be noticed along the top of the plate which could be matched with figure 14 at the 2 millisecond mark. Finally figure 30 (d) shows non-laminar flow conditions are existing over the length of the picture. The thermocouple gage was situated on the bottom of the plate, however, the photographs are indicative of growth not only on the top of the plate but the bottom as well.

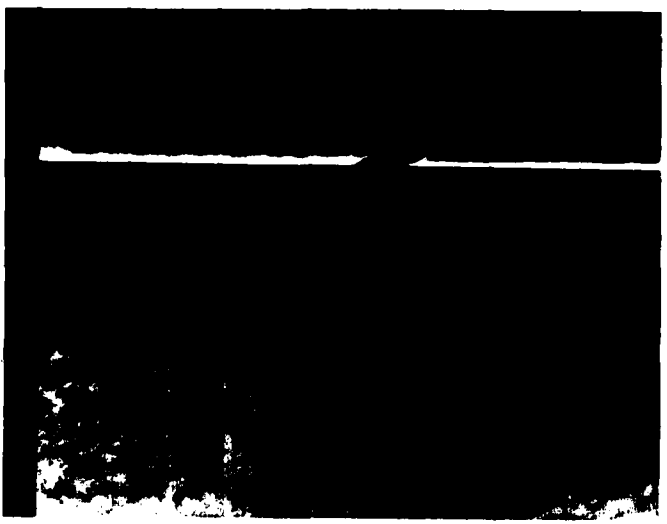


Fig. 31(a)

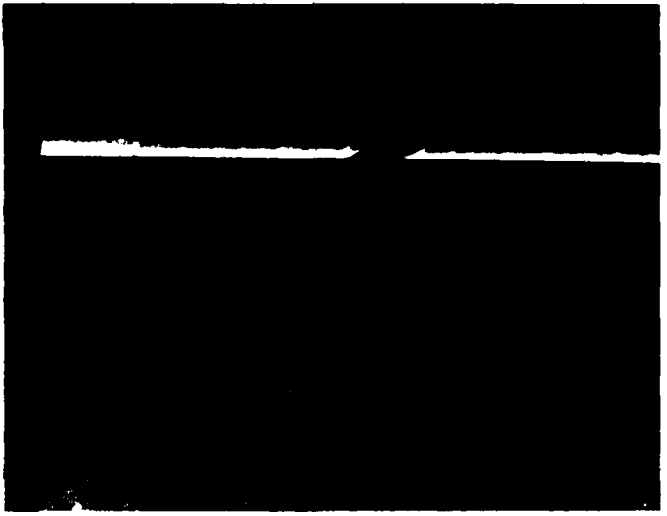


Fig. 31(b)

Figure 31a,b: Boundary Layer Visualization

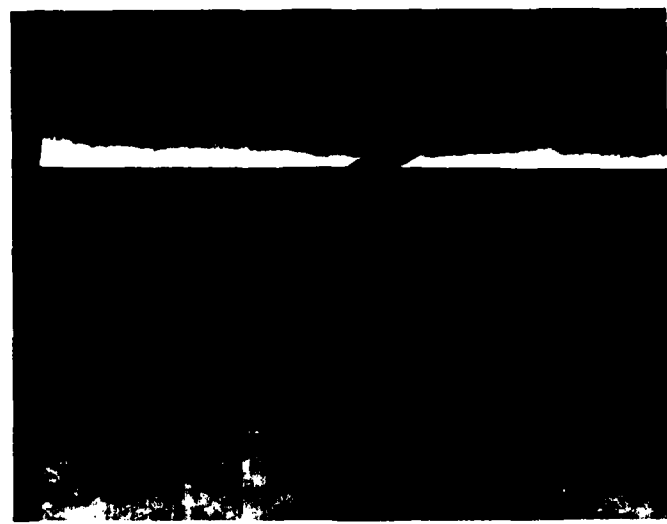


Fig. 31(c)

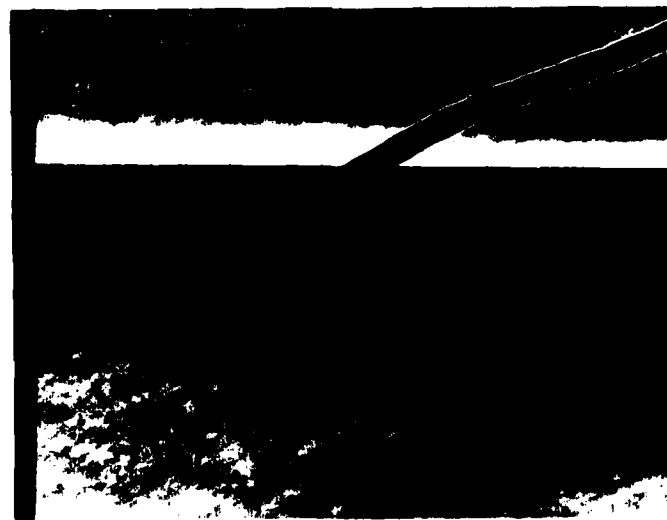


Fig. 31(d)

Figure 31c,d: Boundary Layer Visualization

## VI. Conclusions

The results of this study lead to the following conclusions:

1. Comparison of the heat transfer data for a flat plate behind a traveling normal shock wave with the theoretical solution verified the experimental procedure used during this investigation.
2. The experimental data for the flat plate verified the existence of a transition region between the laminar and turbulent boundary layers. The time of transition agreed with theory which stated that for all intents and purposes the laminar boundary layer reached its asymptotic state at  $\alpha=0.3$ .
3. Heat transfer measurements along the suction side of the turbine vane indicated a decrease in the chordwise direction until the three quarter chord position was reached. The heat transfer at the three quarter chord was indicative of a separation region on the trailing edge of the vane.
4. Schlieren photographs of the flow over a flat plate revealed a thickening of the boundary layer and transition from laminar to turbulent flow.

## VII. Recommendations

The results of this investigation warrant additional study. Further work should be encouraged not only to improve the apparatus and instrumentation, but also to pursue more advanced turbine blade heat transfer studies using the shock tube. A number of improvements which could lead to valuable information are as follows:

1. Modify the analytical solution taking into account the transition from laminar to turbulent boundary layer growth.
2. Investigate the criteria that would explain the anomaly present in figures 17, 18, and 19 indicating the theoretical turbulent boundary layer equation could be computed different ways with drastic results.
3. Expand the scope of the turbine vane heat transfer measurements to capture the transition of the boundary layer along the suction side vane surface for various flow conditions.
4. Re-examine the heat transfer rate for the suction side of the vane and focus a laser interferometer study near the leading edge and transition locality in order to more completely explain the heat transfer history encountered.
5. Pursue flat plate heat transfer profiles at low mach numbers at various positions from the leading edge.
6. Pursue a more advanced study of film cooling effects by

adding blowing or suction along the vane surface.

All of these studies could be performed using the shock tube.

The subsequent results would be significant to the study of turbine vane heat transfer.

## Appendix A

### The Germanium Surface Thermocouple

The semiconductor surface thermocouple used in this study was developed by the McDonnel Aircraft Company for use in their Hypersonic Impulse Tunnel. Figure 32 presents an isometric view of this type of gage as well as some relevant properties. The n and p doped Germanium combination found in these thermocouples provides a sensitivity about 35 times that of conventional Chromel-Constantan thermocouples (Kendall, 1966). The thermo-electric junction is comprised of a thin, Gold film vapor-deposited over the ends of the Germanium. To protect this junction it has been over-plated with a thin layer of Copper. Contributing to the thermocouple's rapid response time is the fact that this Gold and Copper film is only 10 microns thick. The sensitivity and short response time of these gages make them ideal for use in short duration, shock tube facilities.

The Germanium thermocouples were calibrated at the factory using a specialized apparatus consisting of two water baths. Once statically calibrated, chromel leads were attached and the gage seated in a stainless steel housing using epoxy cement. the leakage resistance from the Germanium to the steel case for such a gage was reported to be greater than 10 megaohms while the resistance of the gage used was 380 ohms (Kendall, 1966)

Sensitivity            1.02 mv/°F

Properties of Germanium at 75 F:

Density                332 lbm/cu.ft.  
Specific Heat           0.074 Btu/lbm-°F  
Thermal Conductivity   36 Btu/ft-hr-°F

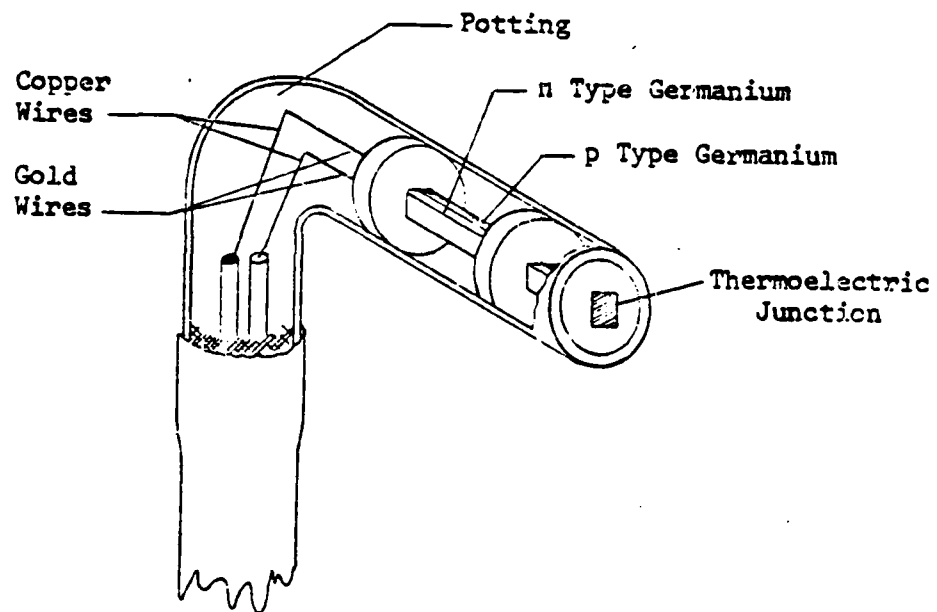


Figure 32: Germanium Surface Thermocouple (Kendall, 1968)

### Appendix B: Equipment

Item	Manufacturer	Model	Serial No.
Oscilloscope	Textronix	7613	B377669
"	"	"	B377677
Oscilloscope	Textronix	535A	6029274
Dual-Trace Amplifier	Textronix	7A	B224442
"	"	"	B196581
"	"	"	B227484
"	"	"	B224382
Dual-Time Base	Textronix	7B53A	B219865
"	"	"	B218268
Four-Channel Amplifier	Textronix	1A4	B125926
Amplifier Mainframe	Honeywell	A-20R	1080152A67
Amplifiers	Honeywell	A-20B-1	1090361-H66
"	"	"	1090362-H66
"	"	"	1090363-H66
"	"	A-20B-34	1090571-C67
"	"	"	1090570-C67
"	"	"	1090567-C67
Delay Generator	Cordin	435	4-608
Power Supply	Kepco	KG25-0.2	A:46394
Spark Lamp	Cordin	5401	6-256
Power Supply	Hewlett-Packard	6205B	1949A16623
Power Supply	Endevco	4225	AC12
Signal Conditioner	Endevco	4423	AE82
"	"	"	AF02
Computer	Hewlett-Packard	85	233A12452
Digitizer	Hewlett-Packard	9874A	1811A01416

## BIBLIOGRAPHY

1. Abbott, D.E., J.D. Walker, H.T. Liu. "Recent Developments in Shock Tube Research," Proceedings of the 9th International Shock Tube Symposium. Stanford University, 1973.
2. AGARDograph 23. "Optical Methods for Examining the Flow in High-Speed Wind Tunnels." NATO 1956
3. Blasius, H. "Grenzschichten in Flüssigkeiten mit kleiner Reibung." Z.Math Phys.56 1-37, 1908. English trans. in NACA TM 1256.
4. Bogdan, Leonard. "Thermal and Electrical Properties of Thin-Film Resistance Gages Used for Heat Transfer Measurement", AIAA Journal. September 1963.
5. Bogdan, Leonard and Joseph E. Garberoglio. Transient Heat Transfer Measurement with Thin-Film Resistance Thermometers -Fabrication and Application technology. Technical Report AFAPL-TR-67-72. Cornell Aeronautical Laboratory, Inc. June 1967.
6. Cook, W. J. and W. J. Felderman. "Reduction of Data from Thin-Film Heat-Transfer Gages: A Concise Numerical Technique", AIAA Journal. March, 1966.
7. Davies, W.R. and L. Berstein. "Heat transfer and transition to turbulence in the shock-induced boundary layer on a semi-infinite flat plate." J. Fluid Mech., Vol 36. part 1, 1969.
8. Dunn, Michael G. Heat Flux and Pressure Measurements and Comparison with Prediction for a Low Aspect Ratio Turbine Stage. Technical Report AFWAL-TR-85-2044. Calspan Advances Technology Center, Buffalo NY. July 1985.
9. Dunn, Michael G. Measurement of Heat Flux and/Pressure in a Turbine Stage. Technical Report AFWAL-TR-81-2055. Calspan Advanced Technology Center. July 1981.
10. Dunn, Michael G. and Frank J. Stoddard. Studies of Heat Transfer to Gas Turbine Components. Technical Report AFAPL-TR-77-66. Calspan Corporation, Buffalo NY. October, 1977.
11. Eckert, E.R.G. and Richard J. Goldstein. Measurements in

Heat Transfer (Second Edition). New York: McGraw-Hill Book Company, 1976.

12. Felderman, E.J. "Heat Transfer and Shear Stress in the Shock-Induced Unsteady Boundary Layer on a Flat Plate." AIAA Journal, Vol 6. no. 3, 1968.
13. Frye, John William. Thin-Film Heat Transfer Gages. Masters Thesis. School of Engineering, Air Force Institute of Technology (AU), Wright-Patterson AFB OH. March 1966.
14. Gaydon, A.G. and I.R. Hurle. The Shock Tube In High-Temperature Chemical Physics. New York: Reinhold Publishing Corporation, 1963.
15. Glass, I.I. "Shock Tubes, Part I: Theory and Performance of Simple Shock Tubes." Utia Review No. 12. Toronto, Canada: Institute of Aerophysics, University of Toronto, 1958.
16. Gochenaur, John E. Investigation of Heat Transfer to a Turbine Blade Cascade Using a Shock Tube. Masters Thesis, GAE-84D. School of Engineering. Air Force Institute of Technology (AU), Wright-Patterson AFB OH, December 1984.
17. Hartunian,R., A. Russo and P.Marrone. Boundary Layer Transition and Heat Transfer in Shock Tubes. Cornell. Heat Transfer and Fluid Mechanics Institute, Stanford University Press. 1958.
18. Jones, T.V. and D.L. Shultz. "Film Cooling Studies in Subsonic and Supersonic Flows Using a Shock Tunnel", Shock Tube Research, Proceedings of the 8th International Shock Tube Symposium, Imperial College, London 5-8 July 1971. Edited by J.L. Stollery, A.G. Gaydon and P.R. Owen. London:Chapman and Hall, 1971.
19. Kendall, David N. and Edward H. Schulte. "Semi-Conductor Surface Thermocouples and Heat-Flux Sensors". Engineering Laboratories, McDonnell Company. April, 1968.
20. Kays, W.M. and M.E. Crawford. Convective Heat and Mass Transfer. New York: McGraw-Hill Book Company, 1980.
21. Mirels, H. "Boundary layer behind shock or thin expansion wave moving into stationary fluid." NACA TN 37 12, 1956.
22. Schlichting, Hermann. Boundary Layer Theory (Seventh Edition). New-York: McGraw-Hill Book Company, 1979.

23. Shapiro, Ascher H. The Dynamics and Thermodynamics of Compressible Fluid Flow, Volume 2. New York: The Ronald Press Company, 1954
23. Stanek, 1Lt. Personal communication regarding the STAN 5 calculations. WPAFB/ASD, November 1985.
24. Zucrow, Maurice and Joe D. Hoffman. Gas Dynamics, Volume 1. New York: John Wiley and Sons, 1976.

Vita

Patrick K. Fillingim was born 14 February 1958 in Spokane Washington, the son of William R. and Helen J. Fillingim. He attended Gonzaga Preparatory High School in Spokane and graduated in 1976. He enrolled in the University of Notre Dame, South Bend IN, fall of 1976. On May 17 1980, he was commissioned a second lieutenant in the United States Air Force completing the Air Force R.O.T.C. program at Notre Dame. The following day he graduated from the University with a Bachelor of Science in Mechanical Engineering, (Nuclear Option). His first assignment was with the Air Force Weapons Laboratory at Kirtland AFB, New Mexico. Lt. Fillingim accepted a regular appointment in the USAF in July 1982. Capt. Fillingim entered the Air Force Institute of Technology in June 1984.

Permanent Address:

N. 5004 Cannon

Spokane, Wash 99205

**UNCLASSIFIED**

SECURITY CLASSIFICATION OF THIS PAGE

**REPORT DOCUMENTATION PAGE**

1a. REPORT SECURITY CLASSIFICATION <b>UNCLASSIFIED</b>		1b. RESTRICTIVE MARKINGS	
2a. SECURITY CLASSIFICATION AUTHORITY		3. DISTRIBUTION/AVAILABILITY OF REPORT Approved for public release; distribution unlimited	
2b. DECLASSIFICATION/DOWNGRADING SCHEDULE			
4. PERFORMING ORGANIZATION REPORT NUMBER(S) <b>AFIT/GAE/AA/85D-7</b>		5. MONITORING ORGANIZATION REPORT NUMBER(S)	
6a. NAME OF PERFORMING ORGANIZATION <b>School of Engineering</b>	6b. OFFICE SYMBOL <i>(If applicable)</i> <b>AFIT/ENA</b>	7a. NAME OF MONITORING ORGANIZATION	
6c. ADDRESS (City, State and ZIP Code) <b>Air Force Institute of Technology Wright-Patterson AFB, Ohio 45433</b>		7b. ADDRESS (City, State and ZIP Code)	
8a. NAME OF FUNDING/SPONSORING ORGANIZATION <b>A.F. Aeropropulsion Lab.</b>	8b. OFFICE SYMBOL <i>(If applicable)</i> <b>AFWAL/POTC</b>	9. PROCUREMENT INSTRUMENT IDENTIFICATION NUMBER	
8c. ADDRESS (City, State and ZIP Code) <b>Wright-Patterson AFB, Ohio 45433</b>		10. SOURCE OF FUNDING NOS.	
		PROGRAM ELEMENT NO.	PROJECT NO.
		TASK NO.	WORK UNIT NO.
11. TITLE (Include Security Classification) <b>(See Box 19)</b>			
12. PERSONAL AUTHOR(S) <b>Patrick K. Fillingim, B.S., M.B.A., Capt., USAF</b>			
13a. TYPE OF REPORT <b>MS Thesis</b>	13b. TIME COVERED FROM _____ TO _____	14. DATE OF REPORT (Yr., Mo., Day) <b>1985 December</b>	15. PAGE COUNT
16. SUPPLEMENTARY NOTATION			
17. COSATI CODES		18. SUBJECT TERMS (Continue on reverse if necessary and identify by block number) <b>Flat Plate, Turbine Blades, Gas Turbine Nozzles, Cascades Heat Transfer, Shock Tube, Thermal Boundary Layer</b>	
19. ABSTRACT (Continue on reverse if necessary and identify by block number)  Title: <b>FLAT PLATE AND TURBINE VANE CASCADE HEAT TRANSFER INVESTIGATION USING A SHOCK TUBE</b>			
Thesis Chairman: <b>Dr. William C. Elrod</b>		<p><i>Approved for public release: 1AW AFR 190-17</i>  <i>Lynn E. WOLVER</i>  <b>Lynn E. WOLVER</b>          Dean for Research and Professional Development          Air Force Institute of Technology (AFIT)          Wright-Patterson AFB OH 45433</p>	
20. DISTRIBUTION/AVAILABILITY OF ABSTRACT  <input checked="" type="checkbox"/> SAME AS RPT. <input type="checkbox"/> DTIC USERS <input type="checkbox"/>		21. ABSTRACT SECURITY CLASSIFICATION <b>UNCLASSIFIED</b>	
22a. NAME OF RESPONSIBLE INDIVIDUAL <b>Dr. William C. Elrod</b>		22b. TELEPHONE NUMBER <i>(Include Area Code)</i> <b>(513) 255-3517</b>	22c. OFFICE SYMBOL <b>AFIT/ENY</b>

UNCLASSIFIED

SECURITY CLASSIFICATION OF THIS PAGE

A shock tube was used to initiate boundary layer growth on a splitter plate at zero incidence. The heat transfer rate determined from a thin film semiconductor gage was compared to theoretical values for the flat plate heat transfer problem. The correlation between the theoretical laminar and turbulent boundary layer equations and the experimental data for various shock Mach number flows showed excellent agreement.

The shock tube was also used to generate high temperature gas flows which were allowed to pass through a turbine vane cascade. Thin film semiconductor and resistance gages were used to provide temperature histories at four locations along the suction side of a turbine vane over a range of shock strengths. Heat transfer rates were determined from these temperature histories using a finite differencing scheme to approximate the energy equation for a semi-infinite solid. The investigation showed that the rate of heat transfer along the suction side of the vane decreased with chordwise position from the stagnation point at the leading edge to the half chord position. At the three quarter chord position, the heat transfer rates were found to be higher than the preceding chord position.

Flow visualization was provided using a schlieren system. Photographs were taken showing boundary layer transition from laminar to turbulent flow for sonic flows over a flat plate

UNCLASSIFIED

SECURITY CLASSIFICATION OF THIS PAGE

**END**

**FILMED**

**386**

**DTIC**